Neurocomputing 273 (2018) 281–295

Contents lists available at ScienceDirect

Neurocomputing

journal homepage: www.elsevier.com/locate/neucom

Memristive recurrent neural network

Gerardo Marcos Tornez Xavier, Felipe Gómez Castañeda*, Luis Martín Flores Nava, José Antonio Moreno Cadenas

Center for Research and Advanced Studies of the IPN, Cinvestav-IPN, Electrical Engineering Department, Av. Instituto Politécnico Nacional 2508, CP 07360 Mexico City, Mexico

ARTICLE INFO

Article history:
Received 8 November 2016
Revised 5 August 2017
Accepted 7 August 2017
Available online 18 August 2017

Communicated by Duan Shukai

Keywords:
Memristor
Team model
Neural network
Hopfield
Continuous-time signal
Analog VLSI design

ABSTRACT

It is reported a continuous-time neural network in CMOS that uses memristors. These nanodevices are used to achieve some analog functions such as constant current sourcing, decaying term emulation, and resistive connection; all of them representing parameters of the neural network. The expected dynamics of this silicon circuit with these functional memristors is demonstrated via SPICE simulations based on 0.5 µm, n-well CMOS technology. The neural circuit is operative by finding the optimal solution of small-size combinatorial optimization problems, namely: "Assignment" and "Transportation". It was chosen fast switching titanium dioxide memristors, which are modeled with nonlinear window functions and tunneling effect with the TEAM paradigm. This analog network belongs to an early recurrent model, which is electrically redesigned to take into account memristive arrays but keeping its original convergence properties. The behavioral and electrical analysis is done via Simulink-SPICE simulation. The outcome VLSI functional blocks combine both current and voltage to represent the variables in the recurrent model.

1. Introduction

The nonlinear and dynamic *i*– *v* characteristics of the nanoscale memory component or memristor were reported by HP Labs [1]. This electrical component was described earlier in the theoretical work by Chua (see first reference in [1]). The memristor represents a modern focus of attention with various topic avenues: from proposing its technology with different materials [2,3] to introducing it in parallel models of computing approaches with bases in complex systems [4,5]. Furthermore, it is envisaged that the electronic design activity has potential possibilities of creating emerging analog and digital systems [6], where the memristor might be introduced as an innovative element. In the academic context, there are electronic designs oriented to demonstrate analog systems based on the Hopfield network configuration, where the traditional weighting resistive elements can be replaced by memristors. This replacement can be implemented in standard electronic technology. In this direction, works in [7,8] deal with two demonstrative prototypes: a 4-bit ADC converter and an associative memory. Taking in particular the Hopfield model as an optimizer, it can be analyzed according to the manner its energy or cost function is stated. The efficiency to solve linear and nonlinear programming problems [9] is an alternate issue in the study of the Hopfield paradigm. Another recurrent neural network that works as an optimizer and becomes attractive for VLSI integration was presented by Wang [10]. This neural model operates with single-valued resistors with a lateral connectivity pattern among neurons.

In this paper, we solve two combinatorial optimization problems with the electrical recurrent network, working as an optimizer, that was used by Wang, where memristors are utilized to represent analog parameters, both static (permanent in time) and dynamic (decaying in time).

We show standard continuous-time CMOS circuits in analog neurons: unit-gain current amplifiers for computing integrals of aggregated currents and inverters for sigmoid functions. The connection between neurons is made with two-memristor arrays that observe the sense of the current. Simulations of the electrical and analytical response of the memristive network done both in Spice and Simulink, provide numerical reference comparisons; they were nearly similar.

The main topic in the electrical design in this work was concerned with the change of value of the resistance in working memristors, i.e. when a current flows through. The objective of using memristors was achieved in three manners: 1) Keeping the Off-state resistance, i.e. a constant-value reference current was implemented by setting a particular analog voltage at the memris-

* Corresponding author.
E-mail addresses: gtornez@cinvestav.mx (G.M. Tornez Xavier), fgomez@cinvestav.mx, felipegomezcastaneda@gmail.com (F. Gómez Castañeda), lmflores@cinvestav.mx (L.M. Flores Nava), jmoreno@cinvestav.mx (J.A. Moreno Cadenas).

http://dx.doi.org/10.1016/j.neucom.2017.08.008

tors terminals, 2) Combining both Off and On-state resistances in a group of memristors, i.e. a dynamic decaying current source with a predetermined peak value was obtained and, 3) Selecting dynamically one of two memristors, i.e. a constant-value bidirectional resistor was emulated.

2. The memristor and its model for circuit design

At present, the memristor is modeled with high-performance software, reproducing its nonlinear and frequency dependence when continuous-time signals are applied to its two terminals. The suitable electrical relation in circuit design is i–v; for the memristor, it comes from observing the Constitutive Relation [11]; it is reproduced in (1), where ϕ is the magnetic flux and q is the electrical charge.

$$f_M(\phi, q) = 0 \tag{1}$$

Using (1) the memristance or $R(q)$ is defined in (2). Therefore, the i–v function of the memristor is defined in (3).

$$R(q) = \frac{df_M(q)}{dq} \tag{2}$$

$$v = R(q)i \tag{3}$$

The main feature that is drawn from (3) is shown when $i = 0$ at time t_0, then the memristor stores charge and memorizes the last memristance value, e.g. $R = R$ (q at t_0). A generalization of (2) and (3) supports circuit-theoretic properties of the memristor, which are expressed by (4) and (5). Where, $\boldsymbol{x} = (x_1, x_2, \ldots x_n)$ represents a state-variable vector.

$$v = R(\boldsymbol{x}, i) \tag{4}$$

$$\frac{d\boldsymbol{x}}{dt} = \boldsymbol{f}(\boldsymbol{x}, i) \tag{5}$$

Both (4) and (5) have minimal representation by reducing $\boldsymbol{x}$ to a scalar-variable x; the common case is when x measures the relative position of a frontier between two adjacent and variable resistive regions in the fabricated nanomaterial. In principle, a low resistivity region that contains moving oxygen vacancies can displace into the other region of high resistivity due to the flow of current in the memristor. Whether w is the width of the region with oxygen vacancies and D is the width of the memristor, the state-variable is given by $x = w/D$.

Most memristor models approach the i–v function observing a nonlinear ion drift behavior [12] and tunneling [13] as dominant conduction mechanisms. They might provide numerical means of the charge-kinetics identification in nanometric materials. However, computation effective features are preferred in memristive circuit design; the TEAM model itself is suitable [14]. In TEAM, x is introduced by modeling dx/dt. This expression is given in (6) replacing w/D by its complement i.e. $x = 1 - w/D$ or $x = d/D$. Where, $d = D - w$, is the effective width of the tunneling gap.

$$\frac{dx}{dt} = \begin{cases} k_{off}\left(\dfrac{i(t)}{i_{off}} - 1\right)^{\alpha_{off}} f_{off}(x), & 0 < i_{off} < i \quad (6a) \\ 0, & i_{on} < i < i_{off} \quad (6b) \\ k_{on}\left(\dfrac{i(t)}{i_{on}} - 1\right)^{\alpha_{on}} f_{on}(x), & i < i_{on} < 0 \quad (6c) \end{cases}$$

In (6), k_{off}, k_{on}, α_{off}, α_{on}, i_{on} and i_{off} are parameters that fit the model with experimental data. Finally, the i–v relation is nonlinear in x according to (7).

$$v(t) = R_{ON} e^{(\lambda/x_{off} - x_{on})(x - x_{on})}\, i(t) \tag{7}$$

R_{ON} and R_{OFF} are the resistances at $x = x_{on}$ and $x = x_{off}$, respectively, and $\lambda = \ln(R_{OFF}/R_{ON})$. The TEAM model was introduced in the circuit design community and oriented to fast digital systems. These characteristics are useful in the recurrent neural network as can be appreciated further.

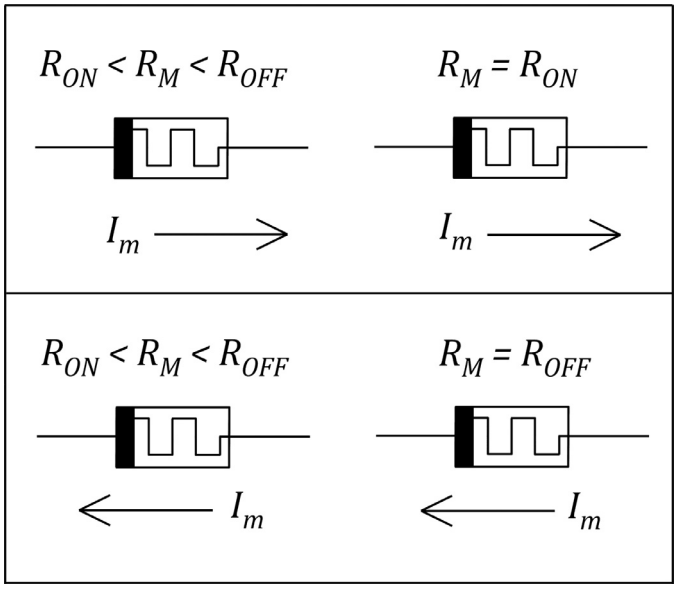

Fig. 1. Memristive states before (left, $R_{ON} < R_M < R_{OFF}$) and after (right, $R_M = R_{ON}$ or $R_M = R_{OFF}$) due to flow of current. This simple procedure sets the values R_{ON} or R_{OFF} in memristors used in the recursive neural network in this work.

3. Memristance for design

The static and dynamic states of the memristor with fast switching features, support the neural network design in this work. The static states are either R_{ON} or R_{OFF} whereas the dynamic states are characterized by dx/dt as a changing resistance. R_{ON} and R_{OFF} are available when the current does not change the direction; therefore, the signal voltage polarity at the memristor terminals should be kept during the analog process. In Fig. 1, the initial resistive states are within the interval $R_{ON} < R_M < R_{OFF}$ (on the left) and the ending states after flowing the current I_m through the memristor (on the right); where R_M is the resistance value of the memristor. For the changing resistance case, when dx/dt is not zero, we take advantage proposing a parallel-series configuration that is suitable to emulate a transient current, whose initial or peak value I_{MS} can represent a parameter of the neural network namely, $\lambda c_{i,j}\exp(-t/\tau)$ which is introduced later. Fig. 2 presents a conceptual diagram of this configuration, where the analog differential potential $(V+)$–$(V-)$ starts to change from zero to V_M at time T_{START}. V_M is an analog voltage that should be found to reach the initial or peak current I_{MS}. Before this transient occurs, the series memristors are in the On-state resistance and the parallel ones in the Off-state resistance. The current through the series memristors causes a change in their individual resistance towards the value R_{OFF}, decreasing I_m down to I_{MF}. Although there are reported analytical expressions that would approximate the transient current I_m, see for example [15], we use the TEAM model to observe that I_m decays from I_{MS} toward I_{MF}. This transient characteristic replaces that one originally described by a discharging capacitor through a resistor in the electrical neural model [10]. Using Ohms Law and considering that there are S_M series memristors and P_M parallel memristors in Fig. 2, the initial (or Peak) and final currents I_{MS} and I_{MF} are given by (8) and (9), respectively.

$$I_{MS} = \frac{V_M}{\left(R_{ON}S_M + \frac{R_{OFF}}{P_M}\right)} \tag{8}$$

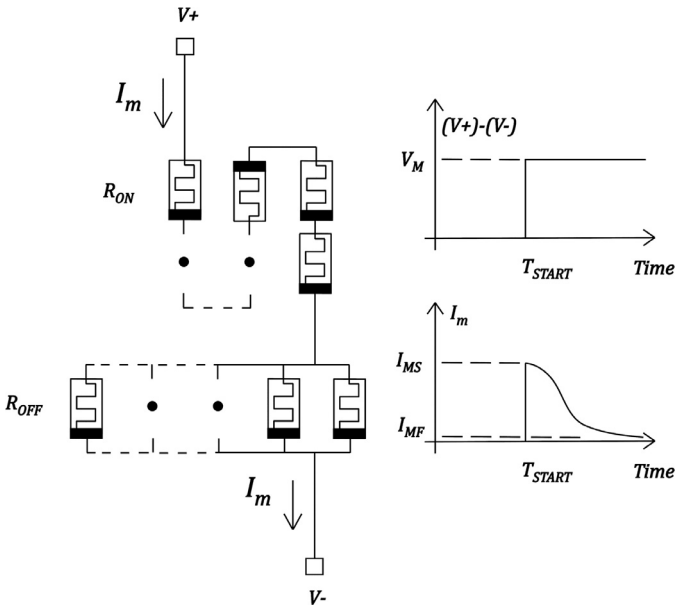

Fig. 2. Transient current in a memristive array. Using S_M series memristors connected with S_P parallel memristors, whose initial memristance is set at R_{ON} and R_{OFF}, respectively, can emulate a decaying current I_m when a voltage step is applied at time T_{START}. The peak current I_{MS} is established according to (8). The final current I_{MF} approaches the value in (9).

$$I_{MF} = \frac{V_M}{\left(R_{OFF}S_M + \frac{R_{OFF}}{P_M}\right)} \tag{9}$$

Changing the number of series or parallel memristors and fixing the voltage difference *(V+)–(V-)*, we can find V_M that satisfies the condition $I_m = I_{MS}$. Finally, as a design constraint, we should observe that *(V+)–(V-)* is limited to an interval.

4. Recurrent neural network

The supporting theory refers to an analog neural network model with n neurons, where the reference neuron N_i recurrently connects the other ones through weighting factors $W_{i,j}$ and whose dynamics ends up solving linear programming problems. The network configuration of this model is built with neurons arranged as a vector, where $W_{i,j}$ with $i, j = 1, 2, \ldots n$ can be represented by a symmetric matrix $\boldsymbol{W}$ as shown in Fig. 3. There exists a self-connection, whose weighting factor is $W_{i,i}$. Using the intermediate variable z_i, the state variable u_i relates with v_j according to (10) and (11), with $i = 1, 2, \ldots$. Therefore, neuron N_i integrates $du_i = z_i dt$, where u_i is the argument of a sigmoid function as denoted in (12) to provide v_i. β is a gain factor.

$$z_i = \frac{du_i}{dt} \tag{10}$$

$$z_i = v_1 W_{i,1} + v_2 W_{i,2} + \ldots v_j W_{i,j} + \ldots v_n W_{i,n} \tag{11}$$

$$v_i = \frac{1}{\left(1 + e^{-\beta u_i}\right)} \tag{12}$$

In particular, for a linear programming problem, whose statement is

Minimize: $f(\boldsymbol{v}) = \boldsymbol{c}^{\mathrm{T}}\boldsymbol{v}$

Subject to: $\boldsymbol{A}\boldsymbol{v} = \boldsymbol{b}$

The matrix $\boldsymbol{W}$ in the recurrent neural network is defined by (13) [16], where η is a positive scalar parameter.

$$\boldsymbol{W} = -\eta \boldsymbol{A}^{\mathrm{T}}\boldsymbol{A} \tag{13}$$

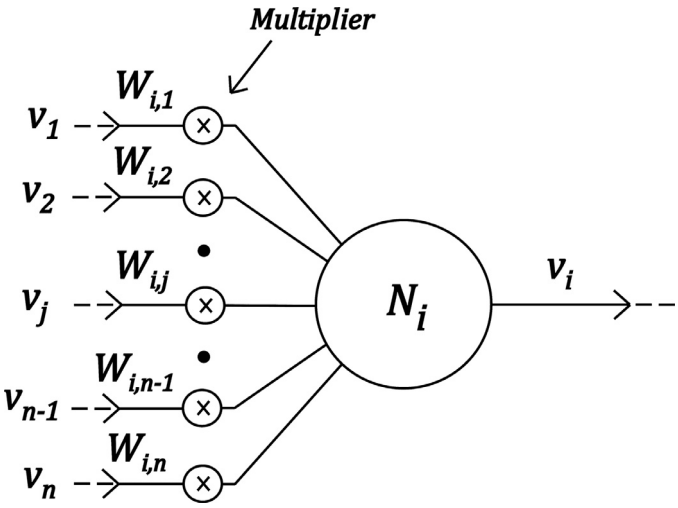

Fig. 3. Neuron N_i for vector array. The input analog signals: v_1, v_2, ..., v_n are multiplied by weighting factors: $W_{i,1}$, $W_{i,2}$, ..., $W_{i,n}$, where they are real numbers. Neuron N_i performs an addition, a temporal integration and a nonlinear transformation.

The entries of $\boldsymbol{A}$ are the coefficients of the linear equations that establish the problem. Additionally, $\boldsymbol{c}$ and $\boldsymbol{b}$ are column vectors of parameters; $\boldsymbol{v}$ is a column vector of the decision variable. The constraint equation might include slack variables where $\{\boldsymbol{b}, \boldsymbol{c}$ and $\boldsymbol{v}\} \in R^n$.

In this case, u_i and v_i are the entries of the column vectors $\boldsymbol{u}$ and $\boldsymbol{v}$ respectively, and they are related according to the state Eq. (14). At the steady state, i.e. $d\boldsymbol{u}/dt = \boldsymbol{0}$, $\boldsymbol{v}$ presents the solution.

$$\frac{d\boldsymbol{u}}{dt} = \boldsymbol{W}\boldsymbol{v} + \eta \boldsymbol{A}^{T}\boldsymbol{b} - \boldsymbol{c}\xi(0)e^{\frac{-t}{\tau}} \tag{14}$$

In (14), the column vector $\boldsymbol{c}$ decays in time due to $\xi(0)exp(-t/\tau)$; where, $\xi(0)$ and τ are the initial (or peak) value and the time constant, respectively.

Wang [16] demonstrated the stability and convergence to near optimal solutions of the recurrent neural network described by the set of equations in (14), which are suitable for circuit implementation in VLSI design. Wang also established a methodology of electrical networks with similar convergence properties in the case of combinatorial optimization problems [10], leading to a matrix of n by n neurons i.e. organized in n rows by n columns. The new network configuration uses neuron, as shown in Fig. 4, in a matrix array, where the factor Q is equal to –1 if $k = i$ or $l = j$, otherwise Q is zero. This factor establishes connections with neurons in the same column and row of the reference neuron $N_{i,j}$. There are only lateral inhibitory connections, all of them having the same value $-W_0$, also there exists a self-connection whose weighting factor is $-2W_0$.

The individual state equations that formulate the "Assignment" problem [17] are given by (15) and (16), where k and l are columns and rows counters, respectively.

$$\frac{du_{i,j}}{dt} = -\eta \sum_{k=1}^{n} v_{i,k} - \eta \sum_{l=1}^{n} v_{l,j} + 2\eta - \lambda c_{i,j} e^{\frac{-t}{\tau}} \tag{15}$$

$$v_{i,j} = \frac{1}{\left(1 + e^{-\beta u_{i,j}}\right)} \tag{16}$$

In (15), the term $-\eta$ that multiplies the summations is the inhibitory weighting factor in the lateral connections; 2η represents a threshold; $c_{i,j}$ belongs to the set of costs in a problem, and decays in time due to $exp(-t/\tau)$ and λ which is a constant. According to our experimental results, it is convenient to replace (16) by

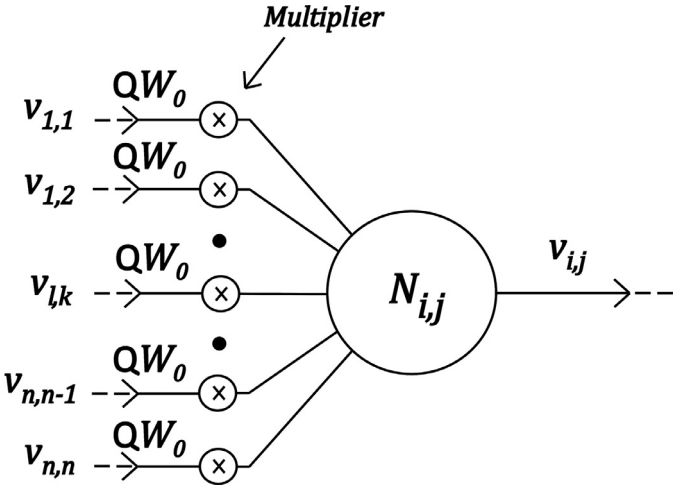

Fig. 4. Neuron $N_{i,j}$ for matrix array. The input analog signals: $v_{1,1}$, $v_{1,2}$, ..., $v_{n,n}$ are multiplied by weighting factors: QW_0, QW_0, ..., QW_0, where, $Q \in \{0, -1\}$ obeys to a lateral connection rule and W_0 is a real positive number. Neuron $N_{i,j}$ performs an addition, a temporal integration and a nonlinear transformation.

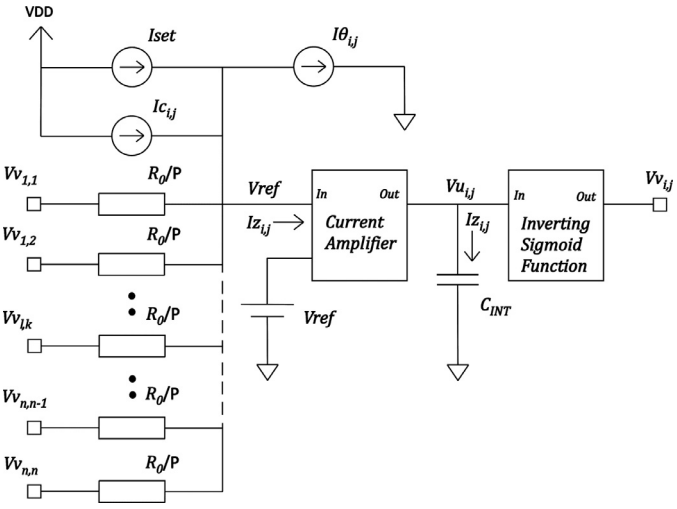

Fig. 5. Electrical configuration of neuron $N_{i,j}$ for matrix array. This system has interconnection resistors R_0/P, where $P \in \{0, 1\}$ obeys to a lateral connection rule. The current amplifier adds the arriving currents at the input node with constant voltage *Vref* to create $Iz_{i,j}$. It is copied and integrated by capacitor C_{INT} to produce $Vu_{i,j}$. Finally, $Vu_{i,j}$ is transformed by the inverting sigmoid function to provide the output voltage $Vv_{i,j}$.

the inverting sigmoid, which is defined in Eq. (17).

$$v_{i,j} = -\frac{1}{\left(1 + e^{-\beta u_{i,j}}\right)} \tag{17}$$

We remark that $c_{i,j}$ and 2η are the entries of new matrices: $\boldsymbol{C}$ and $\boldsymbol{\theta}$, respectively. $c_{i,j}$ and 2η electrically use memristors to encode "Assignment" and "Transportation" problems, treated below as demonstrative applications.

5. Electrical configuration of the neuron

In this section, we show the analog components that build the recurrent neural network, which solves the "Assignment" and "Transportation" problems. In Fig. 5 are shown the processing components in terms of voltage and current variables for the reference neuron $N_{i,j}$ shown in Fig. 4. The weighting factors W_0 are taken as conductances proportional to $1/R_0$, where the set of resistors whose individual value R_0 provides a current that is summed along with *Iset*, $I\theta_{i,j}$ and $Ic_{i,j}$ to form the current $Iz_{i,j}$. This analog variable is entered to the current amplifier with unitary gain, which outputs a replica of $Iz_{i,j}$ to the capacitor C_{INT}. This capacitor works as an integrator of $Iz_{i,j}$ in order to obtain the voltage $Vu_{i,j}$. The inverting sigmoid function reads $Vu_{i,j}$ to produce $Vv_{i,j}$. The current amplifier also copies the voltage *Vref* to its input.

Below is the analytical description of this electrical system that leads to a differential equation that is equivalent to (15), considering that the existing connections are those that fulfill the condition: P is equal to 1 if $k = j$ or $l = i$ (otherwise, $P = 0$ and, there is no connection).

Applying Kirchhoffś Current Law at the input of the current amplifier, $Iz_{i,j}$ is expressed as

$$Iz_{i,j} = \frac{1}{R_0}\sum_{l,k=1}^{n}\left(Vv_{l,k} - Vref\right) + Ic_{i,j} - I\theta_{i,j} + Iset \tag{18}$$

$$Iz_{i,j} = \frac{1}{R_0}\sum_{l,k=1}^{n} Vv_{l,k} - \frac{2nVref}{R_0} + Ic_{i,j} - I\theta_{i,j} + Iset \tag{19}$$

The term $-(2nVref)/R_0$ acts as a bias voltage. Its effect can be reduced to zero by setting *Iset* to

$$Iset = \frac{2nVref}{R_0} \tag{20}$$

Thus, (19) is simplified to

$$Iz_{i,j} = \frac{1}{R_0}\sum_{l,k=1}^{n} Vv_{l,k} + Ic_{i,j} - I\theta_{i,j} \tag{21}$$

We should note that the summation in (21) contains a self-connection, whose value is $2/R_0$.

The next expression after (21) is (22). Where, C_{INT} is the capacitor that integrates $Iz_{i,j}$ to produce $Vu_{i,j}$.

$$\frac{dVu_{i,j}}{dt} = \frac{1}{C_{INT}}\left\{\frac{1}{R_0}\sum_{k=1}^{n} Vv_{i,k} + \frac{1}{R_0}\sum_{l=1}^{n} Vv_{l,j} + Ic_{i,j} - I\theta_{i,j}\right\} \tag{22}$$

(22) is equivalent to (15) but with converse signs on the terms of the right hand side to be taken into consideration with the inverting sigmoid function. Table 1 relates electrical and model parameters.

Table 1
Electrical and model parameters.

$I\theta_{i,j}$	2η	Parameter, constant
$Ic_{i,j}$	$\lambda c_{i,j} e^{\frac{-t}{\tau}}$	Parameter, decaying

The analog input currents $I\theta_{i,j}$ and $Ic_{i,j}$ are the entries of the matrices $\boldsymbol{\theta}$ and $\boldsymbol{C}$, respectively that represent the combinatorial optimization problems in this work.

6. Analog CMOS circuits

We have chosen a low cost standard 0.5 µm, n-well, CMOS technology to design the analog neural network circuits, that were simulated as 3-by-3 matrices of neurons. The power supply VDD is 5 V. The BSIM3v3 MOSFET model electrical parameters of this CMOS technology are provided by ON-Semiconductor to run on the IC-Nanometer Suite by Mentor.

The CMOS circuits that form the Current Amplifier and the Inverting Sigmoid Function are shown in Figs. 6 and 7a, respectively. The W/L ratio of the transistors is shown as µm/µm (this nomenclature applies for all the electrical diagrams). This Current Amplifier is useful for signal processing applications in current-mode designs [18]. It works following the translinear principle of the loop

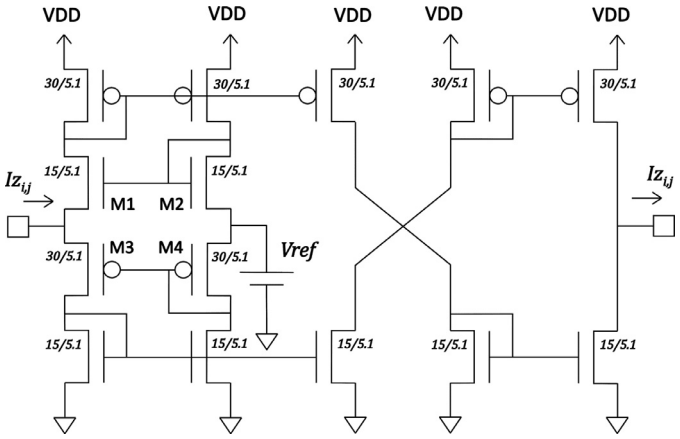

Fig. 6. Current amplifier. This is a current mode analog amplifier designed for unitary gain, where the input current $Iz_{i,j}$ on the left, is provided as a copy on the right.

formed by transistors M1, M2, M3 and M4 transferring *Vref* to the input. It has unitary gain. *Vref* = VDD/2 was chosen. Fig. 7a is a push–pull analog amplifier, whose gain and DC transfer function are set by the transistors size, approximating the inverting nonlinear sigmoid function in (17) and shifting to the first quadrant. Fig. 7b presents $Vv_{i,j}$ versus $Vu_{i,j}$ of the push pull amplifier, where the gain at $Vv_{i,j}$ = VDD/2 is moderate.

7. Memristive components

The TEAM model was implemented with Verilog-A instructions [19]. They were run on the IC-Nanometer Suite by Mentor. Table 2 presents the values of the parameters used in the simulations of the recurrent neural networks. These values correspond to the memristors used whose technology is oriented to fast digital electronics [20]. Using the values in Table 2 and the setup in Fig. 8a, the obtained simulated response is shown in Fig. 8b, where the frequency of the sinusoidal signal covers the range: 1 MHz < f < 3 MHz. Fig. 8c shows applied voltage V_m, memristive current I_m, effective width d and memristance R_M (from top to down) for 1 MHz, 2 MHz and 3 MHz. In Table 2, doing $dt = 1 \times 10^{-9}$ s allows saving computation time. We simulated lots of networks setting their individual integrating capacitors C_{INT} at initial conditions of combinatorial cases of either 0 V or 5 V and choosing the best solution.

Table 2
TEAM parameters used in simulations.

Parameters	Values
dt	1×10^{-9} s
R_{ON}	1×10^{3} ohm
R_{OFF}	500×0^{3} ohm
i_{off}	50×10^{-12} A
i_{on}	-50×10^{-12} A
W_C	107×10^{-12} m
a_{on}	0 m
a_{off}	3×10^{-9} m
k_{on}	-1×10^{-8} m/s
k_{off}	1×10^{-8} m/s
α_{on}	1
α_{off}	1
x_{on}	0 m
x_{off}	3×10^{-9} m

In Fig. 5, the set of resistors, whose number by neuron is $2(n-1)+2$, is composed by memristors with a resistive value: $R_0 = R_{OFF}$ namely, in the Off-state resistance. This condition demands that the sense of the flowing current never changes, whatever its magnitude is; however, we note that the sense of the signal current flow in any memristor might change. Fig. 9 depicts the actual memristive circuit that emulates a constant R_{OFF} for the reference connection between $Vv_{l,k}$ and *Vref*. There, two memristors are selected by a "comparator", which is formed by a chain of 4 digital inverters, whose threshold is *Vref* by design. Memristors MEMR1 and MEMR2 work always in the Off-state resistance. They are selected alternatively when $Vv_{l,k} > Vref$ and $Vv_{l,k} < Vref$, by the transmission gates TG1 and TG2, respectively. TG1 and TG2 are operated by opposite logic levels due to Va and Vb.

Both *Iset* and $I\theta_{i,j}$ provide constant currents and have similar circuit configuration, which also uses memristors in the Off-state resistance. Figs. 10 and 11 show the implementation of the circuits for *Iset*/2 and $I\theta_{i,j}$ respectively, where the difference VDD – *Vref*

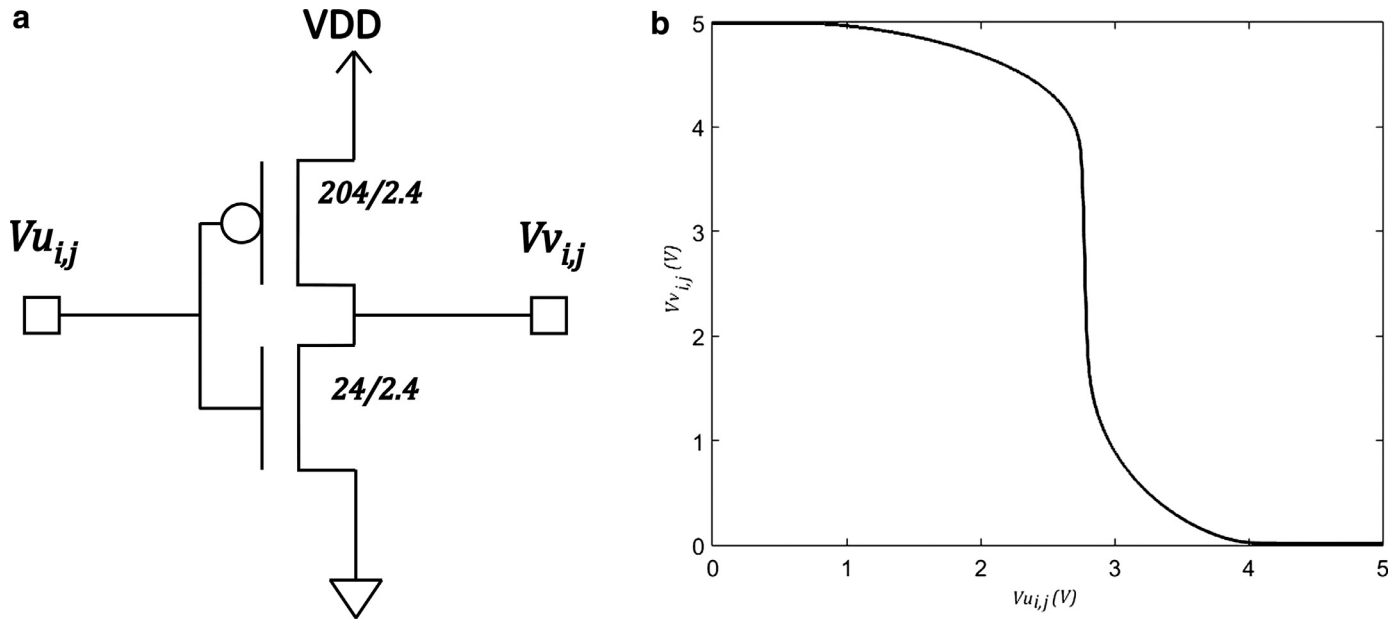

Fig. 7. a. Inverting sigmoid function. This is a push–pull CMOS amplifier that approximates (17). b. Simulation in DC of the inverting sigmoid function.

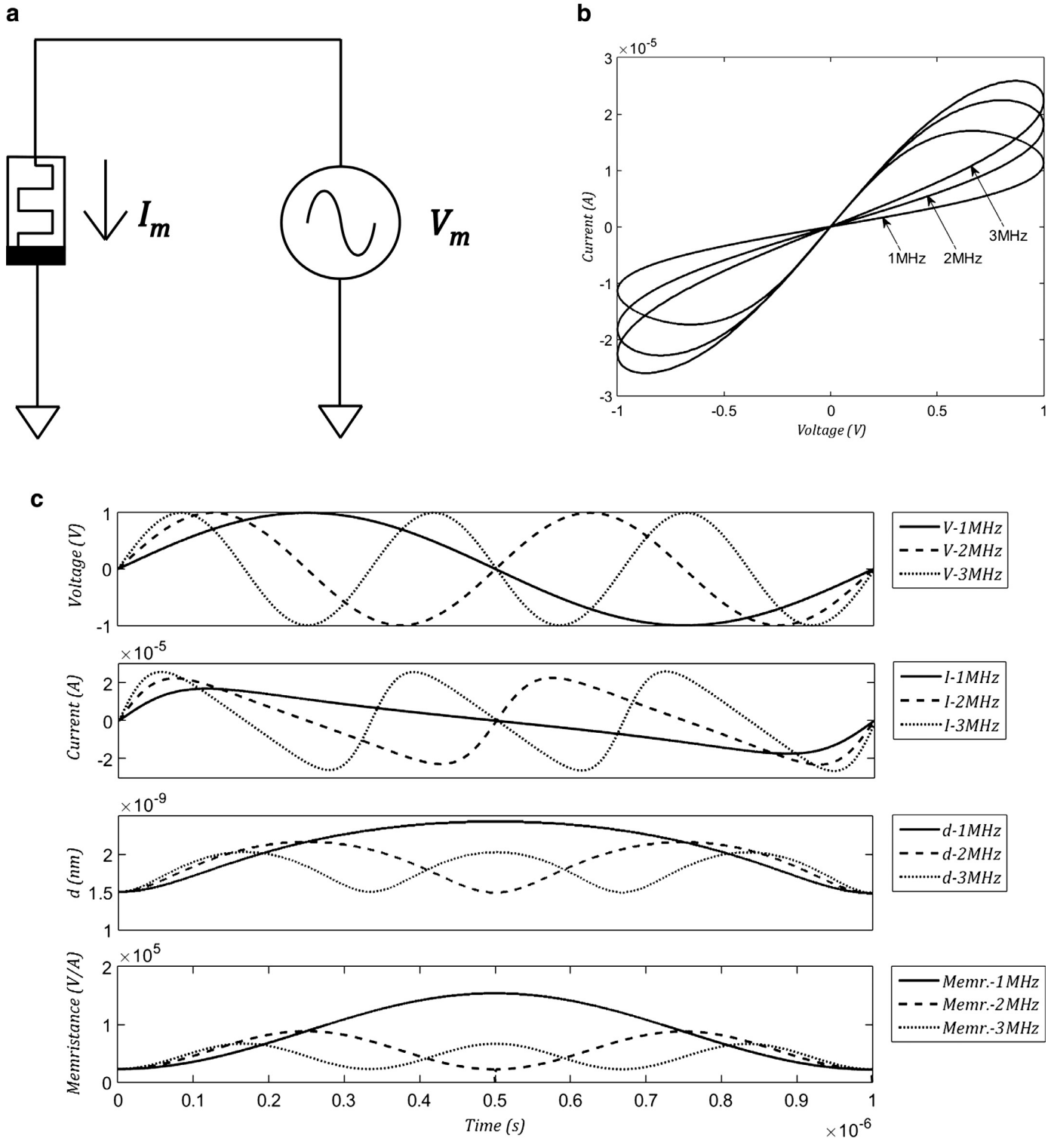

Fig. 8. a. Setup for simulating the $i-v$ characteristic of the memristor. b. Simulation of the $i-v$ characteristic of the memristor with frequency as parameter. c. Simulation as function of time. Top to down graphs: Applied sinusoidal voltage V_m, Current I_m, Effective width d, Memristance R_m.

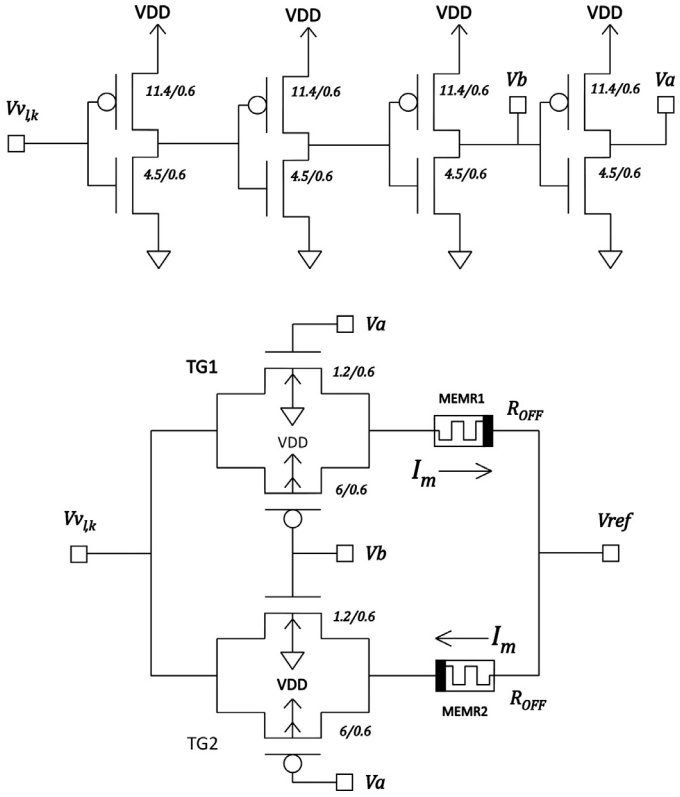

Fig. 9. Circuit for emulating the resistive connection $R_0 = R_{OFF}$ between neurons. Upper diagram: The chain of 4 digital inverters acts as a comparator to the analog voltage $Vv_{i,k}$. The logic threshold of each inverter is set to *Vref* by design. Lower diagram: Switched paths between $Vv_{i,k}$ and *Vref* due to transmission gates TG1 and TG2 that avoid change of sense of current in MEMR1 and MEMR2 and keep them at R_{OFF}. The digital voltages *Va* and *Vb* for controlling TG1 and TG2 come from the comparator (chain of 4 inverters).

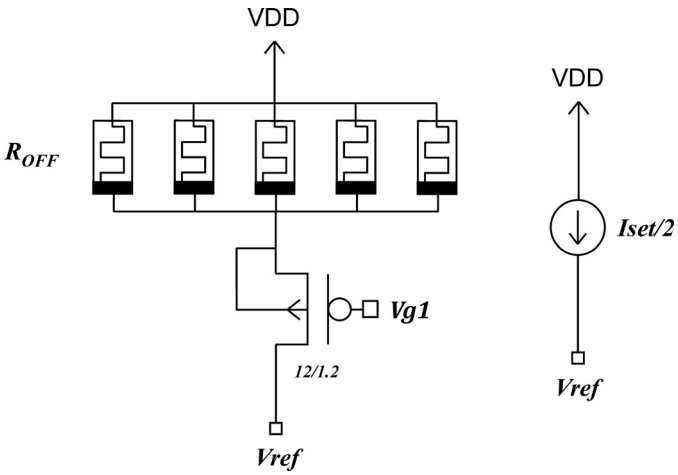

Fig. 10. Current source *Iset*/2. It is implemented using 5 parallel memristors in the R_{OFF} state in series with a p-channel MOS transistor. The analog voltage *Vg*1 sets the current.

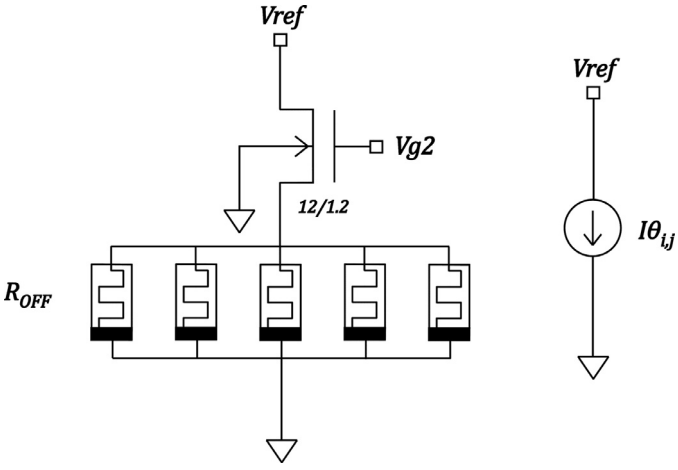

Fig. 11. Current source $I\theta_{i,j}$. It is implemented using 5 parallel memristors in the R_{OFF} state in series with an n-channel MOS transistor. The analog voltage *Vg*2 sets the current.

takes part of the design. This memristive strategy reduces active electronics to a minimal and gets a high output resistance. Based on the electrical simulation, *Vg*1 and *Vg*2 are determined for specific DC currents of *Iset*/2 and $I\theta_{i,j}$, which are shown in Fig. 12a

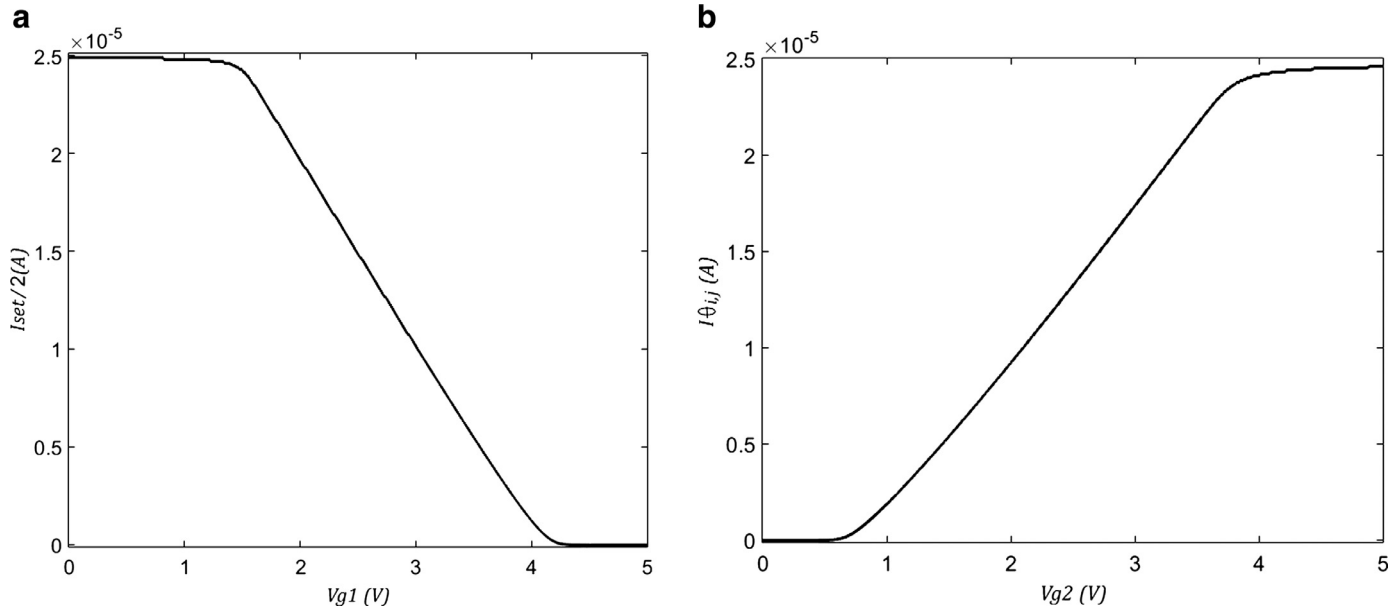

Fig. 12. a. Simulation in DC of *Iset*/2 versus *Vg*1. The useful linear characteristic is in $1.7\,V < Vg1 < 3.85\,V$ for $1.0\,\mu A < Iset/2 < 23.0\,\mu A$, where the circuit in Fig. 10 works properly. b. Simulation in DC of $I\theta_{i,j}$ versus *Vg*2. The useful linear characteristic is in $1.0\,V < Vg2 < 3.70\,V$ for $1.0\,\mu A < I\theta_{i,j} < 23.0\,\mu A$, where the circuit in Fig. 11 works properly.

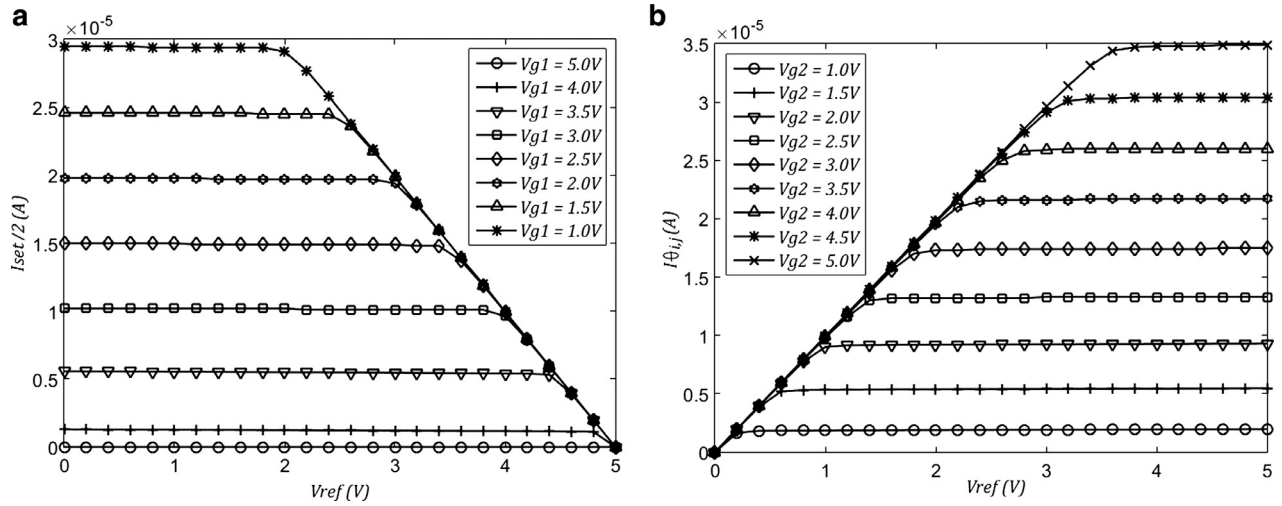

Fig. 13. a. Simulation in DC of *Iset*/2 versus *Vref*, with *Vg*1 as parameter. It is chosen $Vg1 = 2.5\,V$ for $Iset/2 = 15\,\mu A$ and $Vref = 2.5\,V$. These values are used in the neural network. b. Simulation in DC of $I\theta_{i,j}$ versus *Vref*, with *Vg*2 as parameter. *Vg*2 should be chosen in the interval $0.8\,V < Vg2 < 3.5\,V$ to be inside the interval $0\,\mu A < I\theta_{i,j} < 20\,\mu A$. $Vref = 2.5\,V$.

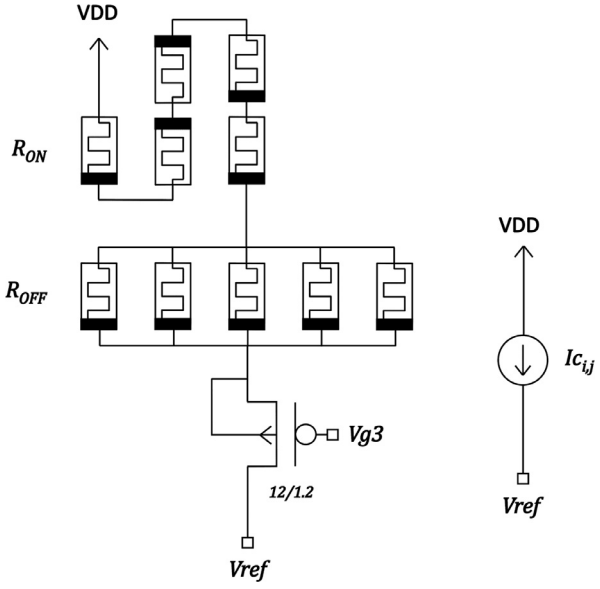

Fig. 14. Current source $Ic_{i,j}$. It is implemented using 5 parallel memristors in the R_{OFF} state in series with 5 series memristors in the R_{ON} state and a p-channel MOS transistor. The analog voltage *Vg*3 sets the peak current.

and b, respectively. Fig. 13a and b provides evidence that both current sources have high output resistance at the working voltage $Vref = 2.5\,V$. Fig. 14 refers to the circuit configuration of $Ic_{i,j}$, which emulates a decaying current and replaces $\lambda c_{i,j}\exp(-t/\tau)$ in the model presented by Wang. Although there is a series transistor, and (9) predicts a lower final current I_{MF}, its decaying characteristic is still suitable. The analog voltage *Vg*3 sets the initial amplitude of the current or the peak current; this value is determined using (8), where $V_M = V_M(Vg3)$ and $S_M = 5$, $P_M = 5$. The I–V DC characteristic is drawn in Fig. 15a. Whether the values 2 μA, 4 μA, 6μA and 10 μA are chosen as the peak currents, the corresponding values of *Vg*3 are 3.74 V, 3.48 V, 3.24 V, 3.00 V and 2.76 V. The transient outcome, with these peak currents is shown in Fig. 15b. In the circuits that approach the currents *Iset*/2, $I\theta_{i,j}$ and $Ic_{i,j}$ the source terminal of the series transistor sets the voltage across the corresponding memristive array following to *Vg*1, *Vg*2 and *Vg*3, respectively. At this point, Fig. 10 deserves noting that it is designed for *Iset*/2 due to functionality reason namely, the series p-MOS transistor works properly. The actual current source *Iset* is implemented by two parallel circuits providing a current equals to *Iset*/2 each.

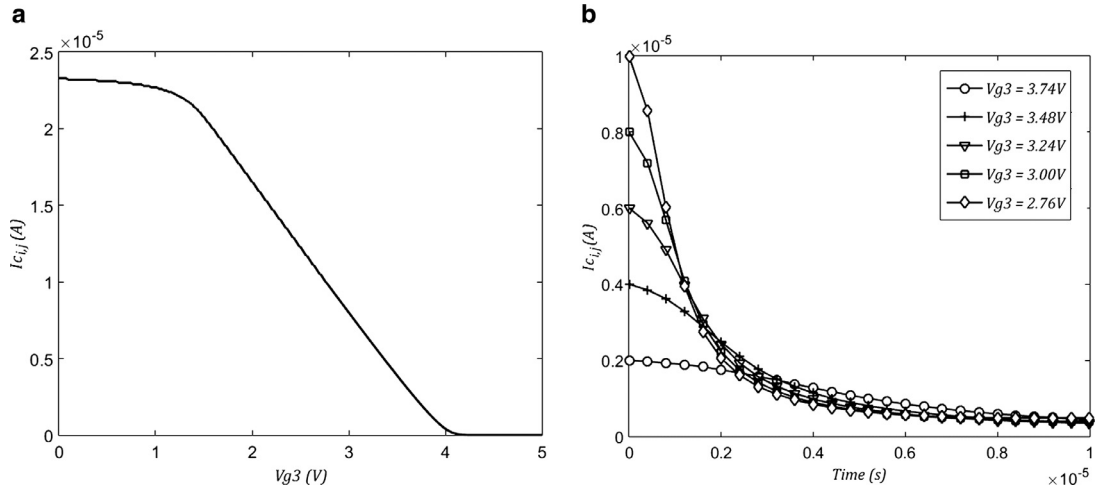

Fig. 15. a. Simulation in DC of $Ic_{i,j}$ versus *Vg*3. The peak current $Ic_{i,j}$ can be set in the interval $1.0\,\mu A < Ic_{i,j} < 20\,\mu A$ corresponding to the interval $1.5\,V < Vg3 < 3.9\,V$, where the circuit in Fig. 14 works properly. b. Simulation of $Ic_{i,j}$. The peak current is set with *Vg*3. From Fig. 15a, the values: $Ic_{i,j} = 10\,\mu A$, 8 μA, 6 μA, 4 μA, and 2 μA are set using $Vg3 = 2.76\,V$, 3.0 V, 3.24 V, 3.48 V and 3.74 V, respectively.

Table 3-A
Numerical costs and electrical currents.

Neuron (i,j)	Netwk1 $C_{i,j}$	Netwk2 $C_{i,j}$	Netwk3 $C_{i,j}$	Netwk1 $I_{Ci,j}$	Netwk2 $I_{Ci,j}$	Netwk3 $I_{Ci,j}$
(1, 1)	7	1	8	7.77	1.11	8.88
(1, 2)	6	7	6	6.66	7.77	6.66
(1, 3)	8	3	1	8.88	3.33	1.11
(2, 1)	9	6	4	9.99	6.66	4.44
(2, 2)	4	5	3	4.44	5.55	3.33
(2, 3)	3	4	5	3.33	4.44	5.55
(3, 1)	5	4	5	5.55	4.44	5.55
(3, 2)	8	6	2	8.88	6.66	2.22
(3, 3)	6	9	9	6.66	9.99	9.99

Table 3-B
Analog and numerical solutions.

Neuron (i,j)	Analog solution $V_{vi,j}$			Numerical solution		
	Netwk1	Netwk2	Netwk3	Netwk1	Netwk2	Netwk3
(1, 1)	0.58382	4.22076	0.03629	0	1	0
(1, 2)	3.97953	0.01529	0.01471	1	0	0
(1, 3)	0.31686	0.60430	4.74946	0	0	1
(2, 1)	0.02195	0.01533	4.04663	0	0	1
(2, 2)	0.71387	0.79085	0.81807	0	0	0
(2, 3)	4.17154	4.07552	0.01708	1	1	0
(3, 1)	4.30346	0.59964	0.81689	1	0	0
(3, 2)	0.19650	4.08336	4.02668	0	1	1
(3, 3)	0.32928	0.22205	0.01484	0	0	0

8. Analog solution of the "Assignment" problem

In this section, we present the solution of "Assignment" problems using the memristive recurrent neural network. Considering Fig. 5 for a 3-by-3 system of neurons, Eq. (20) evaluated for $Vref = VDD/2 = 2.5\,V$, $R_0 = R_{OFF} = 500 \times 10^3$ Ohm, which is implemented with the circuit configuration of Fig. 10, leads to a value of $Iset = 30$ μA. The value of the integrating capacitor C_{INT} is 2.3 pF, which is proposed as 1.0 pF by design in parallel with 1.3 pF due to the gate capacitances of the inverting sigmoid function. The value of the threshold current source $I\theta_{i,j}$ is constant and the same for all neurons, which is established as $I\theta_{i,j} = 20$ μA. In Table 3-A are shown the numerical costs and their respective electrical currents $Ic_{i,j}$ in μA of 3 "Assignment" problems identified as Netwk1, Netwk2 and Netwk3. Table 3-B shows their analog solution in volts along with the expected numerical solution. Fig. 16a, b and c presents the electrical traces $Vv_{i,j}$ of Netwk1, Netwk2 and Netwk3 based on the SPICE simulations. Comparing the analog solution with the numerical solution, we observe that both are equal, considering that if $Vv_{i,j}$ is nearly 5 V or 0 V, it is read as "1" or "0", respectively. Appendix A presents an algebraic analysis of the "Assignment" problem for completeness.

9. Analog solution of the "Transportation" problem

In this section, we present the solution of "Transportation" problems using the memristive recurrent neural network. Considering Fig. 5 for a 3-by-3 system of neurons, Eq. (20) evaluated for $Vref = VDD/2 = 2.5\,V$, $R_0 = R_{OFF} = 500 \times 10^3$ Ohm, which is implemented with the circuit configuration of Fig. 10, leads to a value of $Iset = 30$ μA. The value of the integrating capacitor C_{INT} is 2.3 pF, which is proposed as 1.0 pF by design in parallel with 1.3 pF due to the gate capacitances of the inverting sigmoid function. In Table 4-A are shown the numerical costs, and the offer and demand values of 3 "transportation" problems, identified as Netwk4, Netwk5 and Netwk6. Table 4-B presents the current in μA of the corresponding values of Table 4-A. $I\bar{c}_{i,j}$, $I\bar{a}_i$, and $I\bar{b}_j$ are calculated

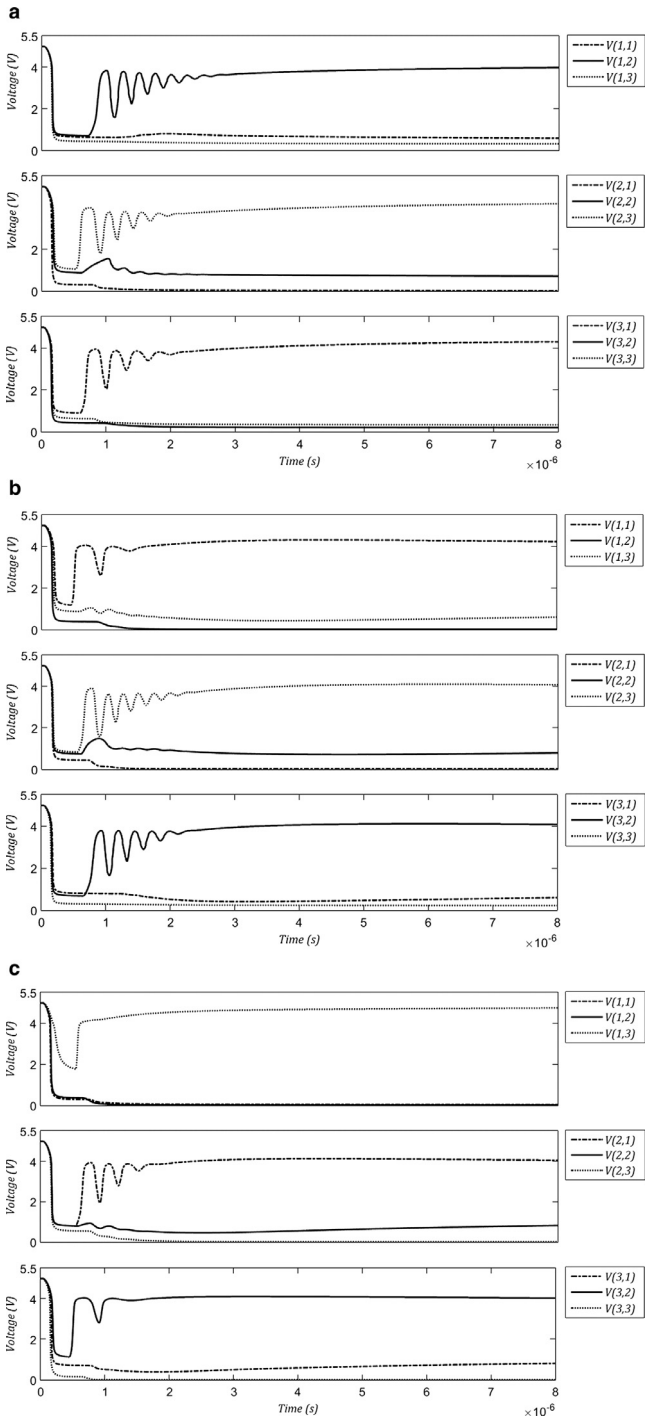

Fig. 16. a. Simulation of Netwk1. b. Simulation of Netwk2. c. Simulation of Netwk3.

Table 4-A
Numerical costs, and offer and demand values.

Neuron (i,j)	Netwk4			Netwk5			Netwk6		
	$C_{i,j}$	a_i	b_j	$C_{i,j}$	a_i	b_j	$C_{i,j}$	a_i	b_j
(1, 1)	7	40	25	7	70	50	8	40	30
(1, 2)	6	40	35	4	70	80	6	40	80
(1, 3)	8	40	60	15	70	45	1	40	10
(2, 1)	9	50	25	1	90	50	4	60	30
(2, 2)	4	50	35	19	90	80	3	60	80
(2, 3)	3	50	60	2	90	45	5	60	10
(3, 1)	5	30	25	3	15	50	5	20	30
(3, 2)	8	30	35	12	15	80	2	20	80
(3, 3)	6	30	60	10	15	45	9	20	10

Table 4-B
Electrical currents.

Neuron (i,j)	Netwk4				Netwk5				Netwk6			
	$I\bar{c}_{i,j}$	$I\bar{a}_i$	$I\bar{b}_j$	I_θ	$I\bar{c}_{i,j}$	$I\bar{a}_i$	$I\bar{b}_j$	I_θ	$I\bar{c}_{i,j}$	$I\bar{a}_i$	$I\bar{b}_j$	I_θ
(1, 1)	7.77	6.66	4.16	10.82	3.684	7.77	5.55	13.32	8.88	5.00	3.75	8.750
(1, 2)	6.66	6.66	5.83	12.49	2.105	7.77	8.88	16.65	6.66	5.00	10.0	15.00
(1, 3)	8.88	6.66	10.0	16.66	7.894	7.77	5.00	12.77	1.11	5.00	1.25	6.250
(2, 1)	9.99	8.33	4.16	12.49	0.526	10.0	5.55	15.55	4.44	7.50	3.75	11.25
(2, 2)	4.44	8.33	5.83	14.16	10.00	10.0	8.88	18.88	3.33	7.50	10.0	17.50
(2, 3)	3.33	8.33	10.0	18.33	1.052	10.0	5.00	15.00	5.55	7.50	1.25	8.750
(3, 1)	5.55	5.00	4.16	9.16	1.578	1.66	5.55	7.210	5.55	2.50	3.75	6.250
(3, 2)	8.88	5.00	5.83	10.83	6.315	1.66	8.88	10.54	2.22	2.50	10.0	12.50
(3, 3)	6.66	5.00	10.0	15.00	5.263	1.66	5.00	6.660	9.99	2.50	1.25	3.750

Table 4-C
Analog solution.

Neuron (i,j)	Netwk4 $v_{i,j}$ (V)	Netwk5 $v_{i,j}$ (V)	Netwk6 $v_{i,j}$ (V)
(1, 1)	0.40308	0.01490	0.45477
(1, 2)	2.65081	3.85953	1.29839
(1, 3)	0.17217	0.01459	0.64134
(2, 1)	0.01454	2.50312	1.18499
(2, 2)	0.01454	0.01464	2.51945
(2, 3)	4.08842	2.56797	0.01481
(3, 1)	1.58085	0.30123	0.12369
(3, 2)	0.15685	0.47318	1.10332
(3, 3)	0.66717	0.01460	0.01473

as: $I\bar{c}_{i,j} = (c_{i,j}/\max(c_{i,j}))(10\,\mu A)$, $I\bar{a}_i = (a_i/\max(a_i, b_j))(10\,\mu A)$ and, $I\bar{b}_j = (b_j/\max(a_i, b_j))(10\,\mu A)$.

$I\theta$ comes from adding $I\bar{a}_i$ and $I\bar{b}_j$. Table 4-C is the analog solution $v_{i,j}$ in volts from simulations. In Table 4-D $v_{i,j}$ is calculated by $v_{i,j} = (v_{i,j}$ in Volts/(5 volts))$(\max(a_i, b_j))$. The offer a_i and demand b_j values in Table 4-D are computed as $a_i = \Sigma\ v_{i,j}$ with $j = 1,2,3$ and $b_j = \Sigma\ v_{i,j}$ with $i = 1,2,3$. Additionally, the total cost of Netw4, Netwk5 and Netwk6 are calculated as $\Sigma\ (c_{i,j})(v_{i,j})$ with $i, j = 1,2,3$. In Table 4-E are shown the values from numerical simulations with Simulink, where $v_{i,j} = (v_{i,j}$ in Simulink)(5 volts)$(\max(a_i, b_j))$. Fig. 17a, b and c presents the electrical traces $Vv_{i,j}$of Netwk4, Netwk5, and Netwk6 respectively, based on SPICE simulations. The total costs by the memristive neural networks in Table 4-D are lower than those by the numerical solution in Table 4-E. Appendix B presents an algebraic analysis of the "Transportation" problem for completeness.

10. Comment on performance

The starting random state value of the memristors deserves a comment on the performance of the whole system. Setting every memristor at R_{ON} or R_{OFF} should be done before the analog computing cycle begins. Naming T_{SET} as the setting period, T_{SET} should be long enough to change in parallel some memristors from R_{ON} to R_{OFF} and the other ones conversely. From simulations, the smallest value of the computing cycle time is $T_{PROCESS} = 8.0$ µs. Also, from simulations $T_{SET} > 650$ ns. Defining $\mathbf{P} = 100\% \times (T_{PROCESS} - T_{SET})/(T_{PROCESS})$ as a Performance Figure of Merit and using the above numbers, we get $\mathbf{P} = 91\%$. Therefore, this analog system supports an acceptable performance.

11. Conclusions

This paper was motivated by the availability of advanced memristor models for circuit design, in particular the TEAM model. The studied neural network was originally modeled by its author using one-value resistive components and decaying currents, leading to linear resistors and discharging capacitors for its implementation; in contrast, we have proposed memristive/CMOS circuit configurations that behave according to the analog parameters of the neural network, solving in continuous-time mode the optimization problems. For this goal, we have chosen electrical parameter values in the TEAM model that belong to fast switching memristors; their dynamic characteristics are complementary of those used in present analog designs, e.g. slow memristive Hopfield networks. We observe that our electrical system represents an innovative system, where new configuration circuits were introduced.

This work contributes in the VLSI design area by proposing the use of memristors working in one of two memristances R_{OFF} or R_{ON}. This system sustains 3 features, namely: **1**) It does not require any programming electronics but flowing current in the direction indicated in Fig. 1, where the proper polarity in the used memristor is chosen. **2**) Using R_{OFF} simplifies the implementation of the current sources: *Iset* and $I\theta_{i,j}$ namely, reduces transistor count and avoids external analog bias voltages. Observing the model by Dr. Wang given by (22), where the value of the resistive interconnections R_0 is constant, it can be chosen as R_{OFF}. **3**) The parallel (R_{OFF})–series (R_{ON}) configuration presented in Fig. 14 is an original idea

Table 4-D
Analog solution.

Neuron (i,j)	Netwk4			Netwk5			Netwk6		
	$v_{i,j}$	a_i	b_j	$v_{i,j}$	a_i	b_j	$v_{i,j}$	a_j	b_j
(1, 1)	4.8370	38.712	23.981	0.2682	70.002	50.746	7.2763	38.312	28.215
(1, 2)	31.809	38.712	33.866	69.471	70.002	78.752	20.774	38.312	78.738
(1, 3)	2.0660	38.712	59.133	0.2626	70.002	46.748	10.261	38.312	10.734
(2, 1)	0.1745	49.410	23.981	45.056	91.543	50.746	18.959	59.508	28.215
(2, 2)	0.1745	49.410	33.866	0.2635	91.543	78.252	40.311	59.508	78.738
(2, 3)	49.061	49.410	59.133	45.223	91.543	46.748	0.2370	59.508	10.734
(3, 1)	18.970	28.858	23.981	5.4221	14.202	50.546	1.9790	19.867	28.215
(3, 2)	1.8822	28.858	33.866	8.5172	14.202	78.252	17.653	19.867	78.738
(3, 3)	8.0060	28.858	59.133	0.2628	14.202	46.748	0.2357	19.867	10.734
	Total cost = 548.641			Total cost = 547.314			Total cost = 438.397		

Table 4-E
Numerical solution.

Neuron	Netwk4			Netwk5			Netwk6		
(i,j)	$v_{i,j}$	a_i	b_j	$v_{i,j}$	a_i	b_j	$v_{i,j}$	a_i	b_j
(1, 1)	3.7917	39.946	24.938	0.0000	69.930	49.945	0.1541	39.767	29.773
(1, 2)	34.899	39.946	34.971	69.930	69.930	79.919	29.763	39.767	79.803
(1, 3)	1.2559	39.346	59.986	0.0000	69.930	44.995	9.8503	39.767	10.158
(2, 1)	0.0000	49.976	24.938	44.993	89.991	49.945	29.465	59.947	29.773
(2, 2)	0.0718	49.976	34.971	0.0000	89.991	79.919	30.327	59.947	79.803
(2, 3)	49.904	49.976	59.986	44.995	89.991	44.995	0.1541	59.947	10.158
(3, 1)	21.146	29.973	24.938	4.9497	14.939	49.945	0.1541	20.020	29.773
(3, 2)	0.0000	29.973	34.971	9.9899	14.939	79.919	19.712	20.020	79.803
(3, 3)	8.8268	29.973	59.986	0.0000	14.939	44.995	0.1541	20.020	10.158
	Total cost = 554.671			Total cost = 549.428			Total cost = 440.862		

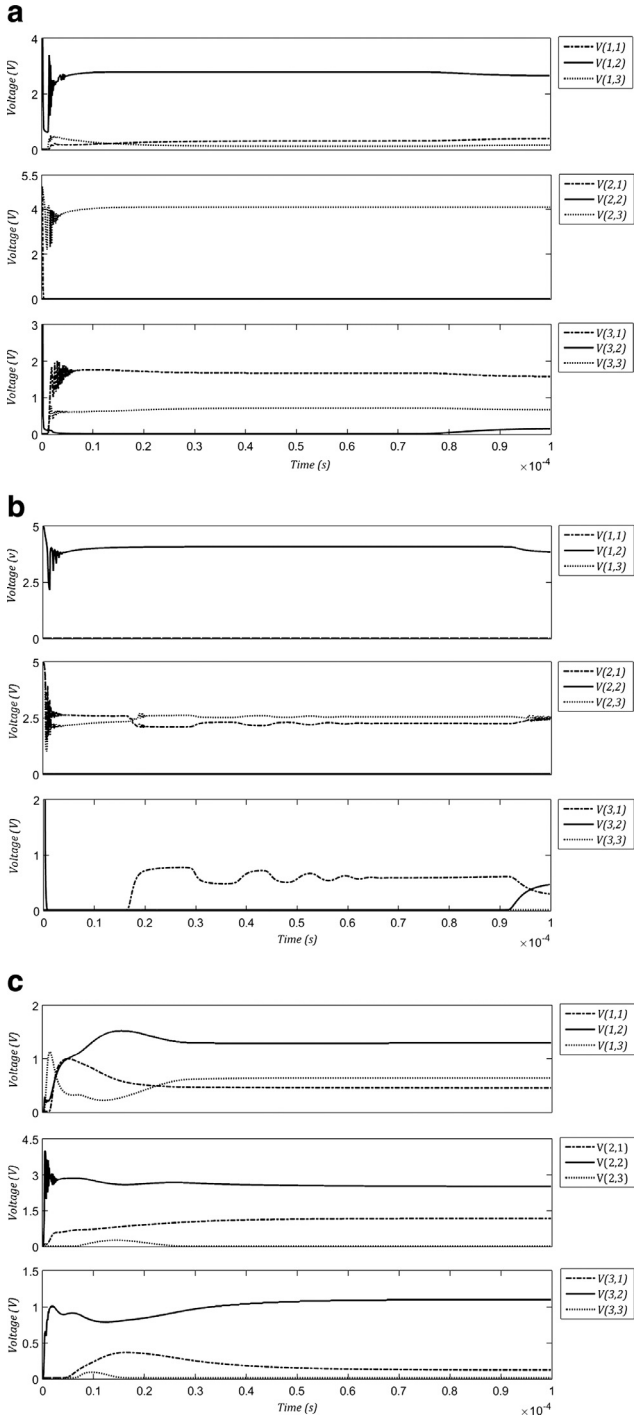

Fig. 17. a. Simulation of Netwk4. b. Simulation of Netwk5. c. Simulation of Netwk6.

of replacing a large capacitive and resistive element to represent the decaying term: $\lambda c_{i,j}\exp(-t/\tau)$ in (15), which is essential to set the parameters of the problem. Alternative ways of interconnecting memristors different from the crossbar architecture, which leads to cellular arrays, support the physical implementation of the analog system in this paper.

Planning in robotics would be a problem for solving by this recurrent neural network. A larger memristive system based on the model by Wang, working as optimizer, is possible by redesigning the CMOS circuits already exposed.

Appendix A

The "Assignment" problem is a linear programming problem, whose description can be associated with the statement:

"There is the need to assign available 'resources' to 'agents' to perform a set of tasks at minimal cost".

This problem is expressed as follows.

$$Minimize\ z = \sum_{i=1}^{n}\sum_{j=1}^{n} c_{ij}v_{ij} \tag{A.1}$$

$$Subject\ to\ \sum_{j=1}^{n} v_{ij} = 1,\ \ i = 1,\ldots,n \tag{A.2}$$

$$\sum_{i=1}^{m} v_{ij} = 1,\ \ j = 1,\ldots,n$$

$$v_{ij} \in \{0,1\},\ \ i,j = 1,\ldots,n; \tag{A.3}$$

where, c_{ij} represents one element of the cost and v_{ij} is the decision variable.

In particular, we obtain the solution to the "Assignment" problem for a 3-by-3 system, using the recurrent neural network by Wang [10]. The mathematical formulation of the supporting analog neural network is

$$\frac{du_{ij}(t)}{dt} = -\eta\sum_{k=1}^{n} v_{ik}(t) - \eta\sum_{l=1}^{n} v_{lj}(t) + 2\eta - \ \lambda c_{ij}e^{-\frac{t}{\tau}} \tag{A.4}$$

$$v_{ij} = g\big(u_{ij}(t)\big) \tag{A.5}$$

where, η and λ are constants. $g(.)$ is a sigmoid function, providing the solution is in the range $[0,1]$.

Eqs. (A.1)–(A.3) for the case of a 3-by-3 system are now represented by:

$$Minimize\ z = \sum_{i=1}^{3}\sum_{j=1}^{3} c_{ij}v_{ij} \tag{A.6}$$

$$Subject\ to\ \sum_{j=1}^{3} v_{ij} = 1,\ \ i = 1,\ldots,3 \tag{A.7}$$

$$\sum_{i=1}^{3} v_{ij} = 1, \quad j = 1, \ldots, 3$$

$$v_{ij} \in [0,\ 1],\ \ i = 1, \ldots, 3;\ \ j = 1, \ldots, 3 \tag{A.8}$$

Eqs. (A.6)–(A.9) get a matrix form as follows

$$Minimize\ z = \boldsymbol{c}^T \boldsymbol{v} \tag{A.9}$$

$$Subject\ to\ \boldsymbol{A}\boldsymbol{v} = \boldsymbol{b} \tag{A.10}$$

Eq. (A.10) can be developed for the 3-by-3 system, to have

$$Minimize\ z = [c_{11}\ c_{12}\ \ c_{13}\ \ c_{21}\ c_{22}\ \ c_{23}\ \ c_{31}\ c_{32}\ \ c_{33}] \begin{bmatrix} v_{11} \\ v_{12} \\ v_{13} \\ v_{21} \\ v_{22} \\ v_{23} \\ v_{31} \\ v_{32} \\ v_{33} \end{bmatrix} \tag{A.11}$$

Eq. (A.11) uses matrix $\boldsymbol{A}$ and vector $\boldsymbol{b}$ as follows, also for the 3-by-3 system.

$$\boldsymbol{A} = \begin{bmatrix} I & I & I \\ B_1 & B_2 & B_3 \end{bmatrix} \tag{A.12}$$

$$\boldsymbol{A} = \begin{bmatrix} 1 & 0 & 0 & 1 & 0 & 0 & 1 & 0 & 0 \\ 0 & 1 & 0 & 0 & 1 & 0 & 0 & 1 & 0 \\ 0 & 0 & 1 & 0 & 0 & 1 & 0 & 0 & 1 \\ 1 & 1 & 1 & 0 & 0 & 0 & 0 & 0 & 0 \\ 0 & 0 & 0 & 1 & 1 & 1 & 0 & 0 & 0 \\ 0 & 0 & 0 & 0 & 0 & 0 & 1 & 1 & 1 \end{bmatrix} \tag{A.13}$$

$$\boldsymbol{b} = \begin{bmatrix} 1 \\ 1 \\ 1 \\ 1 \\ 1 \\ 1 \end{bmatrix} \tag{A.14}$$

Finally, the set of restrictions are expressed as

$$\boldsymbol{A}\boldsymbol{v} = \boldsymbol{b} \tag{A.15}$$

$$\begin{bmatrix} 1 & 0 & 0 & 1 & 0 & 0 & 1 & 0 & 0 \\ 0 & 1 & 0 & 0 & 1 & 0 & 0 & 1 & 0 \\ 0 & 0 & 1 & 0 & 0 & 1 & 0 & 0 & 1 \\ 1 & 1 & 1 & 0 & 0 & 0 & 0 & 0 & 0 \\ 0 & 0 & 0 & 1 & 1 & 1 & 0 & 0 & 0 \\ 0 & 0 & 0 & 0 & 0 & 0 & 1 & 1 & 1 \end{bmatrix} \begin{bmatrix} v_{11} \\ v_{12} \\ v_{13} \\ v_{21} \\ v_{22} \\ v_{23} \\ v_{31} \\ v_{32} \\ v_{33} \end{bmatrix} = \begin{bmatrix} 1 \\ 1 \\ 1 \\ 1 \\ 1 \\ 1 \end{bmatrix} \tag{A.16}$$

$$v_{11} + v_{21} + v_{31} = 1 \tag{A.17}$$

$$v_{12} + v_{22} + v_{32} = 1 \tag{A.18}$$

$$v_{13} + v_{23} + v_{33} = 1 \tag{A.19}$$

$$v_{11} + v_{12} + v_{13} = 1 \tag{A.20}$$

$$v_{21} + v_{22} + v_{23} = 1 \tag{A.21}$$

$$v_{31} + v_{32} + v_{33} = 1 \tag{A.22}$$

The set of differential Eq. (A.4) has its matrix form given as

$$\frac{d\boldsymbol{u}(t)}{dt} = -\eta\left(\boldsymbol{W}v - \boldsymbol{\theta}\right) - \lambda \boldsymbol{c} e^{-\frac{t}{\tau}} \tag{A.23}$$

The matrix of weights $\boldsymbol{W}$ is defined as

$$\boldsymbol{W} = \boldsymbol{A}^T \boldsymbol{A} \tag{A.24}$$

$$\mathrm{W} = \begin{bmatrix} 2 & 1 & 1 & 1 & 0 & 0 & 1 & 0 & 0 \\ 1 & 2 & 1 & 0 & 1 & 0 & 0 & 1 & 0 \\ 1 & 1 & 2 & 0 & 0 & 1 & 0 & 0 & 1 \\ 1 & 0 & 0 & 2 & 1 & 1 & 1 & 0 & 0 \\ 0 & 1 & 0 & 1 & 2 & 1 & 0 & 1 & 0 \\ 0 & 0 & 1 & 1 & 1 & 2 & 0 & 0 & 1 \\ 1 & 0 & 0 & 1 & 0 & 0 & 2 & 1 & 1 \\ 0 & 1 & 0 & 0 & 1 & 0 & 1 & 2 & 1 \\ 0 & 0 & 1 & 0 & 0 & 1 & 1 & 1 & 2 \end{bmatrix} \tag{A.25}$$

The threshold matrix $\boldsymbol{\theta}$ is given as

$$\boldsymbol{\theta} = \boldsymbol{A}^T \boldsymbol{b} \tag{A.26}$$

$$\theta = \begin{bmatrix} 1 & 0 & 0 & 1 & 0 & 0 \\ 0 & 1 & 0 & 1 & 0 & 0 \\ 0 & 0 & 1 & 1 & 0 & 0 \\ 1 & 0 & 0 & 0 & 1 & 0 \\ 0 & 1 & 0 & 0 & 1 & 0 \\ 0 & 0 & 1 & 0 & 1 & 0 \\ 1 & 0 & 0 & 0 & 0 & 1 \\ 0 & 1 & 0 & 0 & 0 & 1 \\ 0 & 0 & 1 & 0 & 0 & 1 \end{bmatrix} \begin{bmatrix} 1 \\ 1 \\ 1 \\ 1 \\ 1 \\ 1 \end{bmatrix} \tag{A.27}$$

$$\theta = \begin{bmatrix} 2 \\ 2 \\ 2 \\ 2 \\ 2 \\ 2 \end{bmatrix} \tag{A.28}$$

Replacing matrices W y θ in the below matrix form, where λ is defined as: $1/c_{max}$, we get for the 3-by-3 system, the below algebraic analysis:

$$\frac{d\boldsymbol{u}(t)}{dt} = -\eta\left(\boldsymbol{W}\boldsymbol{v} - \boldsymbol{\theta}\right) - \lambda \boldsymbol{c} e^{-\frac{t}{\tau}} \tag{A.29}$$

$$\frac{d\boldsymbol{u}(t)}{dt} = -\eta \left(\begin{bmatrix} 2 & 1 & 1 & 1 & 0 & 0 & 1 & 0 & 0 \\ 1 & 2 & 1 & 0 & 1 & 0 & 0 & 1 & 0 \\ 1 & 1 & 2 & 0 & 0 & 1 & 0 & 0 & 1 \\ 1 & 0 & 0 & 2 & 1 & 1 & 1 & 0 & 0 \\ 0 & 1 & 0 & 1 & 2 & 1 & 0 & 1 & 0 \\ 0 & 0 & 1 & 1 & 1 & 2 & 0 & 0 & 1 \\ 1 & 0 & 0 & 1 & 0 & 0 & 2 & 1 & 1 \\ 0 & 1 & 0 & 0 & 1 & 0 & 1 & 2 & 1 \\ 0 & 0 & 1 & 0 & 0 & 1 & 1 & 1 & 2 \end{bmatrix} \times \begin{bmatrix} v_{11} \\ v_{12} \\ v_{13} \\ v_{21} \\ v_{22} \\ v_{23} \\ v_{31} \\ v_{32} \\ v_{33} \end{bmatrix} - \begin{bmatrix} 2 \\ 2 \\ 2 \\ 2 \\ 2 \\ 2 \end{bmatrix} \right) - \lambda \begin{bmatrix} c_{11} e^{-\frac{t}{\tau}} \\ c_{12} e^{-\frac{t}{\tau}} \\ c_{13} e^{-\frac{t}{\tau}} \\ c_{21} e^{-\frac{t}{\tau}} \\ c_{22} e^{-\frac{t}{\tau}} \\ c_{23} e^{-\frac{t}{\tau}} \\ c_{31} e^{-\frac{t}{\tau}} \\ c_{32} e^{-\frac{t}{\tau}} \\ c_{33} e^{-\frac{t}{\tau}} \end{bmatrix} \tag{A.30}$$

$$\frac{du_{11}}{dt} = -2\eta v_{11} - \eta(v_{12} + v_{13}) - \eta(v_{21} + v_{31}) + 2\eta - \lambda C_{11} e^{-\frac{t}{\tau}} \tag{A.31}$$

$$\frac{du_{12}}{dt} = -2\eta v_{12} - \eta(v_{11} + v_{13}) - \eta(v_{22} + v_{32}) + 2\eta - \lambda C_{12} e^{-\frac{t}{\tau}} \tag{A.32}$$

$$\frac{du_{13}}{dt} = -2\eta v_{13} - \eta(v_{11} + v_{12}) - \eta(v_{23} + v_{33}) + 2\eta - \lambda C_{13} e^{-\frac{t}{\tau}} \tag{A.33}$$

$$\frac{du_{21}}{dt} = -2\eta v_{21} - \eta(v_{22} + v_{23}) - \eta(v_{11} + v_{31}) + 2\eta - \lambda C_{21} e^{-\frac{t}{\tau}} \tag{A.34}$$

$$\frac{du_{22}}{dt} = -2\eta v_{22} - \eta(v_{21} + v_{23}) - \eta(v_{12} + v_{32}) + 2\eta - \lambda C_{22} e^{-\frac{t}{\tau}} \tag{A.35}$$

$$\frac{du_{23}}{dt} = -2\eta v_{23} - \eta(v_{21} + v_{22}) - \eta(v_{13} + v_{33}) + 2\eta - \lambda C_{23} e^{-\frac{t}{\tau}} \tag{A.36}$$

$$\frac{du_{31}}{dt} = -2\eta v_{31} - \eta(v_{32} + v_{33}) - \eta(v_{11} + v_{21}) + 2\eta - \lambda C_{31} e^{-\frac{t}{\tau}} \tag{A.37}$$

$$\frac{du_{32}}{dt} = -2\eta v_{32} - \eta(v_{31} + v_{33}) - \eta(v_{12} + v_{22}) + 2\eta - \lambda C_{32} e^{-\frac{t}{\tau}} \tag{A.38}$$

$$\frac{du_{33}}{dt} = -2\eta v_{33} - \eta(v_{31} + v_{32}) - \eta(v_{13} + v_{23}) + 2\eta - \lambda C_{33} e^{-\frac{t}{\tau}} \tag{A.39}$$

Appendix B

The "Transportation" problem, also known as "Distribution" problem is a linear programming problem, whose description can be associated with the statement:

"There is the need to transport units from a site call 'The Source' to other site called 'The Destination' minimizing the cost of sending and at the same time satisfying offer and demand restrictions".

This problem is expressed as follows.

$$Minimize\ z = \sum_{i=1}^{g}\sum_{j=1}^{h} c_{ij} v_{ij} \tag{B.1}$$

$$Subject\ to\ \sum_{j=1}^{h} v_{ij} = a_i,\ \ i = 1, \ldots, g \tag{B.2}$$

$$\sum_{i=1}^{g} v_{ij} = b_j,\ \ j = 1, \ldots, h$$

$$v_{ij} \geq 0,\ \ i = 1, \ldots, g;\ \ j = 1, \ldots, h \tag{B.3}$$

where, c_{ij} represents one element of the cost and v_{ij} is the decision variable. There would be slack components in order to have a square matrix of size n x n.

In particular, we obtain the solution to the "Transportation" problem for a 3-by-3 system, using the recurrent neural network by Wang [10] and following the method proposed in [21]. The mathematical formulation of the supporting analog neural network is

$$\frac{du_{ij}(t)}{dt} = -\eta \sum_{k=1}^{n} \bar{v}_{ik}(t) - \eta \sum_{l=1}^{n} \bar{v}_{lj}(t) + \eta\theta_{ij} - \lambda c_{ij} e^{-\frac{t}{\tau}} \tag{B.4}$$

$$\bar{v}_{ij} = g\big(u_{ij}(t)\big) \tag{B.5}$$

where, η and λ are constants. $g(.)$ is a sigmoid function, providing the solution is in the range $[0, 1]$; therefore, the values of a, b y v in Eqs. (B.1)–(B.3) are also in this range.

Defining: $q = max\{a_i, b_i : i = 1, 2, 3\}$ then, a new set of variables is

$$v = \ q\bar{v}, a = q\bar{a} \text{ y } b = q\bar{b}.$$

Using the new values of a y b, Equations (B.1)–(B.3) for the case of a 3-by-3 system are now represented by

$$Minimize\ z = \sum_{i=1}^{3}\sum_{j=1}^{3} c_{ij} \bar{v}_{ij} \tag{B.6}$$

$$Subject\ to\ \sum_{j=1}^{3} \bar{v}_{ij} = \bar{a}_i,\ \ i = 1, \ldots, 3 \tag{B.7}$$

$$\sum_{i=1}^{3} \bar{v}_{ij} = \bar{b}_j,\ \ j = 1, \ldots, 3$$

$$\bar{v}_{ij} \in [0,\ \ 1],\ \ i = 1, \ldots, 3;\ \ j = 1, \ldots, 3 \tag{B.8}$$

Eqs. (B.7)–(B.10) get a matrix form as follows

$$Minimize\ \bar{z} = \boldsymbol{c}^T \bar{\boldsymbol{v}} \tag{B.9}$$

$$Subject\ to\ \boldsymbol{A}\bar{\boldsymbol{v}} = \boldsymbol{d} \tag{B.10}$$

Eq. (B.11) can be developed for the 3-by-3 system, to have

$$Minimize\ \bar{z} = [c_{11}\ c_{12}\ \ c_{13}\ \ c_{21}\ c_{22}\ \ c_{23}\ \ c_{31}\ c_{32}\ \ c_{33}] \begin{bmatrix} \bar{v}_{11} \\ \bar{v}_{12} \\ \bar{v}_{13} \\ \bar{v}_{21} \\ \bar{v}_{22} \\ \bar{v}_{23} \\ \bar{v}_{31} \\ \bar{v}_{32} \\ \bar{v}_{33} \end{bmatrix} \tag{B.11}$$

Eq. (B.11) uses matrix $\boldsymbol{A}$ and vector $\boldsymbol{d}$ as follows, also for the 3-by-3 system

$$\boldsymbol{A} = \begin{bmatrix} B_1 & B_2 & B_3 \\ I & I & I \\ 0 & 0 & 0 \end{bmatrix} \tag{B.12}$$

$$\mathrm{A} = \begin{bmatrix} 1 & 1 & 1 & 0 & 0 & 0 & 0 & 0 & 0 \\ 0 & 0 & 0 & 1 & 1 & 1 & 0 & 0 & 0 \\ 0 & 0 & 0 & 0 & 0 & 0 & 1 & 1 & 1 \\ 1 & 0 & 0 & 1 & 0 & 0 & 1 & 0 & 0 \\ 0 & 1 & 0 & 0 & 1 & 0 & 0 & 1 & 0 \\ 0 & 0 & 1 & 0 & 0 & 1 & 0 & 0 & 1 \\ 0 & 0 & 0 & 0 & 0 & 0 & 0 & 0 & 0 \\ 0 & 0 & 0 & 0 & 0 & 0 & 0 & 0 & 0 \\ 0 & 0 & 0 & 0 & 0 & 0 & 0 & 0 & 0 \end{bmatrix} \tag{B.13}$$

$$\boldsymbol{d} = \begin{bmatrix} \bar{a} \\ \bar{b} \\ 0 \end{bmatrix} \tag{B.14}$$

$$\boldsymbol{d} = \begin{bmatrix} \bar{a}_1 \\ \bar{a}_2 \\ \bar{a}_3 \\ \bar{b}_1 \\ \bar{b}_2 \\ \bar{b}_3 \\ 0 \\ 0 \\ 0 \end{bmatrix} \tag{B.15}$$

Finally, the offer and demand restrictions are expressed as

$$\boldsymbol{A}\bar{\boldsymbol{v}} = \boldsymbol{d} \tag{B.16}$$

$$\begin{bmatrix} 1 & 1 & 1 & 0 & 0 & 0 & 0 & 0 & 0 \\ 0 & 0 & 0 & 1 & 1 & 1 & 0 & 0 & 0 \\ 0 & 0 & 0 & 0 & 0 & 0 & 1 & 1 & 1 \\ 1 & 0 & 0 & 1 & 0 & 0 & 1 & 0 & 0 \\ 0 & 1 & 0 & 0 & 1 & 0 & 0 & 1 & 0 \\ 0 & 0 & 1 & 0 & 0 & 1 & 0 & 0 & 1 \\ 0 & 0 & 0 & 0 & 0 & 0 & 0 & 0 & 0 \\ 0 & 0 & 0 & 0 & 0 & 0 & 0 & 0 & 0 \\ 0 & 0 & 0 & 0 & 0 & 0 & 0 & 0 & 0 \end{bmatrix} \begin{bmatrix} \bar{v}_{11} \\ \bar{v}_{12} \\ \bar{v}_{13} \\ \bar{v}_{21} \\ \bar{v}_{22} \\ \bar{v}_{23} \\ \bar{v}_{31} \\ \bar{v}_{32} \\ \bar{v}_{33} \end{bmatrix} = \begin{bmatrix} \bar{a}_1 \\ \bar{a}_2 \\ \bar{a}_3 \\ \bar{b}_1 \\ \bar{b}_1 \\ \bar{b}_1 \\ 0 \\ 0 \\ 0 \end{bmatrix} \tag{B.17}$$

$$\bar{v}_{11} + \bar{v}_{12} + \bar{v}_{13} = \bar{a}_1 \tag{B.18}$$

$$\bar{v}_{21} + \bar{v}_{22} + \bar{v}_{23} = \bar{a}_2 \tag{B.19}$$

$$\bar{v}_{31} + \bar{v}_{32} + \bar{v}_{33} = \bar{a}_3 \tag{B.20}$$

$$\bar{v}_{11} + \bar{v}_{21} + \bar{v}_{31} = \bar{b}_1 \tag{B.21}$$

$$\bar{v}_{12} + \bar{v}_{22} + \bar{v}_{32} = \bar{b}_2 \tag{B.22}$$

$$\bar{v}_{13} + \bar{v}_{23} + \bar{v}_{33} = \bar{b}_3 \tag{B.23}$$

The set of differential equation (*B*.4) has its matrix form given as

$$\frac{d\boldsymbol{u}(t)}{dt} = -\eta\left(\boldsymbol{W}\bar{\boldsymbol{v}} - \boldsymbol{\theta}\right) - \lambda \boldsymbol{c} e^{-\frac{t}{\tau}} \tag{B.24}$$

The matrix of weights $\boldsymbol{W}$ is defined as

$$\boldsymbol{W} = \boldsymbol{A}^T\boldsymbol{A} \tag{B.25}$$

$$\mathbf{W} = \begin{bmatrix} 2 & 1 & 1 & 1 & 0 & 0 & 1 & 0 & 0 \\ 1 & 2 & 1 & 0 & 1 & 0 & 0 & 1 & 0 \\ 1 & 1 & 2 & 0 & 0 & 1 & 0 & 0 & 1 \\ 1 & 0 & 0 & 2 & 1 & 1 & 1 & 0 & 0 \\ 0 & 1 & 0 & 1 & 2 & 1 & 0 & 1 & 0 \\ 0 & 1 & 0 & 1 & 2 & 1 & 0 & 1 & 1 \\ 1 & 0 & 0 & 1 & 0 & 0 & 2 & 1 & 1 \\ 0 & 1 & 0 & 0 & 1 & 0 & 1 & 2 & 1 \\ 0 & 0 & 1 & 0 & 0 & 1 & 1 & 1 & 2 \end{bmatrix} \tag{B.26}$$

The offer and demand limits are related by matrix $\boldsymbol{\theta}$ as

$$\boldsymbol{\theta} = \boldsymbol{A}^T\boldsymbol{d} \tag{B.27}$$

$$\theta = \begin{bmatrix} 1 & 0 & 0 & 1 & 0 & 0 & 0 & 0 & 0 \\ 1 & 0 & 0 & 0 & 1 & 0 & 0 & 0 & 0 \\ 1 & 0 & 0 & 0 & 0 & 1 & 0 & 0 & 0 \\ 0 & 1 & 0 & 1 & 0 & 0 & 0 & 0 & 0 \\ 0 & 1 & 0 & 0 & 0 & 1 & 0 & 0 & 0 \\ 0 & 1 & 0 & 0 & 1 & 0 & 0 & 0 & 0 \\ 0 & 0 & 1 & 1 & 0 & 0 & 0 & 0 & 0 \\ 0 & 1 & 1 & 0 & 1 & 0 & 0 & 0 & 0 \\ 0 & 0 & 1 & 0 & 0 & 1 & 0 & 0 & 0 \end{bmatrix} \begin{bmatrix} \bar{a}_1 \\ \bar{a}_2 \\ \bar{a}_3 \\ \bar{b}_1 \\ \bar{b}_2 \\ \bar{b}_3 \\ 0 \\ 0 \\ 0 \end{bmatrix} \tag{B.28}$$

$$\theta = \begin{bmatrix} \bar{a}_1 + \bar{b}_1 & \bar{a}_1 + \bar{b}_2 & \bar{a}_1 + \bar{b}_3 \\ \bar{a}_2 + \bar{b}_1 & \bar{a}_2 + \bar{b}_2 & \bar{a}_2 + \bar{b}_3 \\ \bar{a}_3 + \bar{b}_1 & \bar{a}_3 + \bar{b}_2 & \bar{a}_3 + \bar{b}_3 \end{bmatrix} \tag{B.29}$$

Replacing matrices $\boldsymbol{W}$ y $\boldsymbol{\theta}$ in the below matrix form, where λ is defined as: $1/c_{max}$, we get for the 3-by-3 system, the below algebraic analysis.

$$\frac{d\boldsymbol{u}(t)}{dt} = -\eta\left(\boldsymbol{W}\bar{\boldsymbol{v}} - \boldsymbol{\theta}\right) - \lambda \boldsymbol{c} e^{-\frac{t}{\tau}} \tag{B.30}$$

$$\frac{d\boldsymbol{u}(t)}{dt} = -\eta\left(\begin{bmatrix} 2 & 1 & 1 & 1 & 0 & 0 & 1 & 0 & 0 \\ 1 & 2 & 1 & 0 & 1 & 0 & 0 & 1 & 0 \\ 1 & 1 & 2 & 0 & 0 & 1 & 0 & 0 & 1 \\ 1 & 0 & 0 & 2 & 1 & 1 & 1 & 0 & 0 \\ 0 & 1 & 0 & 1 & 2 & 1 & 0 & 1 & 0 \\ 0 & 0 & 1 & 1 & 1 & 2 & 0 & 0 & 1 \\ 1 & 0 & 0 & 1 & 0 & 0 & 2 & 1 & 1 \\ 0 & 1 & 0 & 0 & 1 & 0 & 1 & 2 & 1 \\ 0 & 0 & 1 & 0 & 0 & 1 & 1 & 1 & 2 \end{bmatrix} \begin{bmatrix} \bar{v}_{11} \\ \bar{v}_{12} \\ \bar{v}_{13} \\ \bar{v}_{21} \\ \bar{v}_{22} \\ \bar{v}_{23} \\ \bar{v}_{31} \\ \bar{v}_{32} \\ \bar{v}_{33} \end{bmatrix} - \begin{bmatrix} \bar{a}_1 + \bar{b}_1 \\ \bar{a}_1 + \bar{b}_2 \\ \bar{a}_1 + \bar{b}_3 \\ \bar{a}_1 + \bar{b}_1 \\ \bar{a}_1 + \bar{b}_2 \\ \bar{a}_1 + \bar{b}_3 \\ \bar{a}_1 + \bar{b}_1 \\ \bar{a}_1 + \bar{b}_2 \\ \bar{a}_1 + \bar{b}_3 \end{bmatrix}\right) - \lambda \begin{bmatrix} c_{11}e^{-\frac{t}{\tau}} \\ c_{12}e^{-\frac{t}{\tau}} \\ c_{13}e^{-\frac{t}{\tau}} \\ c_{21}e^{-\frac{t}{\tau}} \\ c_{22}e^{-\frac{t}{\tau}} \\ c_{23}e^{-\frac{t}{\tau}} \\ c_{31}e^{-\frac{t}{\tau}} \\ c_{32}e^{-\frac{t}{\tau}} \\ c_{33}e^{-\frac{t}{\tau}} \end{bmatrix} \tag{B.31}$$

$$\frac{du_{11}}{dt} = -2\eta\bar{v}_{11} - \eta(\bar{v}_{12} + \bar{v}_{13}) - \eta(\bar{v}_{21} + \bar{v}_{31}) + \eta\left(\bar{a}_1 + \bar{b}_1\right) - \lambda C_{11}e^{-\frac{t}{\tau}} \tag{B.32}$$

$$\frac{du_{12}}{dt} = -2\eta\bar{v}_{12} - \eta(\bar{v}_{11} + \bar{v}_{13}) - \eta(\bar{v}_{22} + \bar{v}_{32}) + \eta\left(\bar{a}_1 + \bar{b}_2\right) - \lambda C_{12}e^{-\frac{t}{\tau}} \tag{B.33}$$

$$\frac{du_{13}}{dt} = -2\eta\bar{v}_{13} - \eta(\bar{v}_{11} + \bar{v}_{12}) - \eta(\bar{v}_{23} + \bar{v}_{33}) + \eta\left(\bar{a}_1 + \bar{b}_3\right) - \lambda C_{13}e^{-\frac{t}{\tau}} \tag{B.34}$$

$$\frac{du_{21}}{dt} = -2\eta\bar{v}_{21} - \eta(\bar{v}_{22} + \bar{v}_{23}) - \eta(\bar{v}_{11} + \bar{v}_{31}) + \eta\left(\bar{a}_2 + \bar{b}_1\right) - \lambda C_{21}e^{-\frac{t}{\tau}} \tag{B.35}$$

$$\frac{du_{22}}{dt} = -2\eta\bar{v}_{22} - \eta(\bar{v}_{21} + \bar{v}_{23}) - \eta(\bar{v}_{12} + \bar{v}_{32}) + \eta\left(\bar{a}_2 + \bar{b}_2\right) - \lambda C_{22}e^{-\frac{t}{\tau}} \tag{B.36}$$

$$\frac{du_{23}}{dt} = -2\eta\bar{v}_{23} - \eta(\bar{v}_{21} + \bar{v}_{22}) - \eta(\bar{v}_{13} + \bar{v}_{33}) + \eta\left(\bar{a}_2 + \bar{b}_3\right) - \lambda C_{23}e^{-\frac{t}{\tau}} \tag{B.37}$$

$$\frac{du_{31}}{dt} = -2\eta\bar{v}_{31} - \eta(\bar{v}_{32} + \bar{v}_{33}) - \eta(\bar{v}_{11} + \bar{v}_{21}) + \eta\left(\bar{a}_3 + \bar{b}_1\right) - \lambda C_{31}e^{-\frac{t}{\tau}} \tag{B.38}$$

$$\frac{du_{32}}{dt} = -2\eta\bar{v}_{32} - \eta(\bar{v}_{31} + \bar{v}_{33}) - \eta(\bar{v}_{12} + \bar{v}_{22}) + \eta\left(\bar{a}_3 + \bar{b}_2\right) - \lambda C_{32}e^{-\frac{t}{\tau}} \tag{B.39}$$

$$\frac{du_{33}}{dt} = -2\eta\bar{v}_{33} - \eta(\bar{v}_{31} + \bar{v}_{32}) - \eta(\bar{v}_{13} + \bar{v}_{23}) + \eta\left(\bar{a}_3 + \bar{b}_3\right) - \lambda C_{33}e^{-\frac{t}{\tau}} \tag{B.40}$$

References

[1] D.B. Strukov, G.S. Snider, D.R. Stewart, R.S. Williams, The missing memristor found, Nature 453 (2008) 80–83.
[2] S.K. Tripathi, R. Kaur, M. Rani, Oxide nanomaterials and their applications as a memristor, Solid State Phenom. 222 (2015) 67–97.

[3] N.M. Muhammad, N. Duraisamy, K. Rahman, H.W. Dang, J. Jo, K.H. Choi, Fabrication of printed memory device having zinc-oxide active nano-layer and investigation of resistive switching, Curr. Appl. Phys 13 (2013) 90–96.
[4] Y.V. Pershin, M. Di Ventra, Memcomputing and swarm intelligence, https://arxiv.org/abs/1408.6741.
[5] A. Gelencsér, T. Podromakis, C. Toumazou, T. Roska, Biomimetic model of the outer plexiform layer by incorporating memristive devices, Phys. Rev. E. 85 (2012) 041918-1–041918-10.
[6] S.P. Mohanty, Memristor: from basics to deployment, IEEE Potentials 32 (2013) 34–39.
[7] L. Gao, F. Merrikh-Bayat, F. Alibart, X. Guo, B.D. Hoskins, K.T. Cheng, D.B. Strukov, Digital-to-analog and analog-to-digital conversion with metal oxide memristors for ultra-low power computing, http://ieeexplore.ieee.org/stamp/stamp.jsp?tp=&arnumber=6623031.
[8] S.G. Hu, Y. Liu, Z. Liu, T.P. Chen, J.J. Wang, Q. Yu, L.J. Deng, Y. Yin, S. Hosaka, Associative memory realized by a reconfigurable memristive Hopfield neural network, Nat Commun. 6 (2015) 1–8.
[9] U.P. Wen, K.M. Lan, H.S. Shih, A review of Hopfield neural networks for solving mathematical programming problems, Eur. J. Oper. Res 198 (2009) 675–687.
[10] J. Wang, Analysis and design of an analog sorting network, IEEE Trans. Neural Netw. 6 (4) (1995) 962–971.
[11] A. Adamatzky, L. Chua (Eds.), Memristor Networks, Springer, Switzerland, 2014, pp. 1–13.
[12] T. Prodromakis, B.P. Peh, C. Papavassiliou, C. Toumazou, A versatile memristor model with nonlinear dopant kinetics, IEEE Trans. Electron. Devices 58 (9) (2011) 3099–3105.
[13] M.D. Pickett, D.B. Strukov, J.L. Borghetti, J.J. Yang, G.S. Snider, D.R. Stewart, R.S. Williams, Switching dynamics in titanium dioxide memristive devices, J. Appl. Phys 106 (2009) 0744508-1-0744508-6.
[14] S. Kvatinsky, E.G. Friedman, A. Kolodny, U.C. Weiser, TEAM: threshold adaptive memristor model, IEEE Trans. Circuit Syst. 60 (1) (2013) 211–221.
[15] M.S. Feali, A. Ahmadi, Transient response characteristic of memristor circuits and biological-like current spikes, Neural Comput. Appl. (2016), doi:10.1007/s00521-016-2248-1.
[16] J. Wang, Analysis and design of a recurrent neural network for linear programming, IEEE Trans. Circuit Syst. 40 (9) (1993) 613–618.
[17] J. Wang, Analogue neural network for solving the assignment problem, Electron. Lett. 28 (11) (1992) 1047–1050.
[18] G. Palmisano, G. Palumbo, S. Pennisi, CMOS Current Amplifiers, Springer, USA, 1999, pp. 45–48.
[19] S. Kvatinsky, K. Talisveyberg, D. Fliter, A. Kolodny, U. Weiser, E.G. Friedman, Models of memristors for SPICE simulations, http://ieeexplore.ieee.org/stamp/stamp.jsp?arnumber=6377081.
[20] S. Kvatinsky, N. Wald, G. Satat, A. Kolodny, U.C. Weiser, MRL memristor ratioed logic, http://ieeexplore.ieee.org/stamp/stamp.jsp?tp=&arnumber=6331426.
[21] P.H. Siqueira, Application of Wang's recurrent neural network to solve the transportation problem, Int. J. Comput. Sci. Netw. Secur. 12 (7) (2012) 50–54.

Gerardo Marcos Tornez Xavier. He is a doctoral student in the Electrical Engineering Department of Cinvestav-IPN, Mexico City, Mexico. He studies dynamical properties of fundamental memristive circuits. His academic achievements include designing with FPGA a multilayer neural network for predicting electrical response of solar modules.

Felipe Gómez Castañeda. He is researcher at the Center for Research and Advanced Studies of the IPN, Cinvestav-IPN, Mexico City, Mexico. He teaches neuro-fuzzy systems for digital realization with FPGA and analog VLSI design. His areas of interests include metaheuristics and adaptive systems, memristive hardware, analog realization of Sigma-Delta modulators.

Luis Martín Flores Nava. He is a lecturer at the Center for Research and Advanced Studies of the IPN, Cinvestav-IPN, Mexico City, Mexico. He teaches digital systems for realization with FPGA. His areas of interests include robotic vision systems and memristive hardware.

José Antonio Moreno Cadenas. He is professor at the Center for Research and Advanced Studies of the IPN, Cinvestav-IPN, Mexico City, Mexico. He teaches neuro-fuzzy systems for digital realization and use in robotic systems. His areas of interests include vision systems, data mining for geographical data and analysis of complex systems with fuzzy and neural networks.